SONY

Saving Energy in Cellular IoT using Low-Power Wake-up Radios

Dripta Ray & Ratna Pavan Kumar Ponna

Department of Electrical and Information Technology
Lund University

Supervisor: Nafiseh Mazloum
Assistant Supervisor: Ove Edfors

Examiner: Fredrik Rusek

August 31, 2018

Printed in Sweden
Tryckeriet i E-huset, Lund

Abstract

The thesis work is based on power saving techniques to enhance the battery life of Machine Type Communication devices. The basic principle behind the introduced methods to save energy is to allow the Machine Type Communication devices only to perform its activities for a short time and go to sleep or inactive mode for rest of the time. The existing techniques saves a part of device energy consumption which increases the battery life to some extent. To further improve the battery life of these devices, a low power Wake-up Receiver (WRx) is introduced additionally to wake up the power-hungry main receiver when data transfer is required. We started our analysis by evaluating the average power consumption for the existing solutions and compare them with the scenario where the wake-up receiver is integrated into the device. Different possibilities of the design of wake up signal for a wake-up receiver are studied and proposals are made for its specific use and it needs to be accommodated within the operating bandwidth in accordance with the Long Term Evolution signal parameters. The characteristics of the wake-up receiver which influences the parameters like the probability of miss, detection and false alarm are simulated with the wake-up signal designed and the results show a saving up to ninety-six percent of energy when compared to the reference cases considered in this thesis.

Acknowledgments

This Master's thesis work would not have been possible without the kind support and guidance of our supervisor, Dr. Nafiseh Mazloum and assistant supervisor Prof. Ove Edfors. First of all, we would like to thank Nafiseh for the careful supervision of our work. She has always motivated us and uncomplainingly listened to our queries and showed us the way towards the next milestone. We always found the research papers related to our work readily available, and they were forwarded to us in a very diligent way. She has created a free and friendly atmosphere which helped us approach her easily to clarify our doubts. She has always motivated us to move forward and patiently listened to all our thoughts and explained things logically which helped us to grasp the basics of the research work to a much greater extent.

We felt lucky having Ove as our assistant supervisor and are thankful to him for his guidance and suggestions regarding the bits and pieces of our research work. He has always been adjusting his busy schedule in order to give us more support and time. We never felt any difficulty in reaching him and always felt at ease in communication. He has understood our perspective and made things look much simpler with his problem approach methodologies.

Finally, we would like to thank our families who are far away and show their support, patience and lifted our morale to continue the work successfully.

Dripta Ray & Ratna Pavan Kumar Ponna

Popular Science Summary

This thesis work is about saving energy of *Internet of things* (IoT) devices in the cellular network. With the introduction of IoT, it is foreseen, millions of devices in a smart city will be connected to the cellular network. They are the backbone of control systems in the smart cities. These devices are battery powered and are scattered all over the city and at different approach levels. It is quite a difficult task to maintain the services if the battery runs out at short duration. Replacing the batteries would become a dedicated task in hand, in order to maintain the services. There are two ways to solve this problem, either we provide a battery which lasts long or make the communication more efficient. We have chosen the latter approach as our case study in this thesis work. We tried to find a way, the battery life can be extended by means of reducing unnecessary consumption. We investigate a solution where a low power wake-up receiver is integrated with the existing circuitry of the main receiver and see if it proves to be beneficial in terms of power saving. We design a suitable wake-up signal for this type of arrangement and simulate its performance. The thesis work is based on the idle mode operation of a device when it is configured to any of the two popular energy saving schemes Discontinuous Reception (DRX) and extended Discontinuous Reception (eDRX). We focus on the devices where the amount of data transfer is low and it communicates infrequently with the base station, for example, a temperature sensor. With the addition of the wake-up receiver, a considerable amount of energy can be saved compared to the existing solutions.

Table of Contents

List of Abbreviations

3GPP Third Generation Partnership Project

AFE Analog Front End

CMF Cell-identity Matched Filter

DBB Digital Base Band

DRX Discontinuous Reception

DTX Discontinuous Transmission

eDRX extended Discontinuous Reception

IDS Identity De-Spreader

IoT Internet of Things

LTE Long Term Evolution

LTE-A LTE-Advanced

MCL Maximum Coupling Loss

MPDCCH MTC Physical Downlink Control Channel

P-RNTI Paging Radio Network Temporary Identifier

PCI Physical Cell Identity

PDSCH Physical Downlink Shared Channel

PRACH Physical Random Access Channel

PSM Power Saving Mode

PSS Primary Synchronization Signal

PTW Paging Time Window

ROC Receiver Operational Characteristics

RSS Resynchronization Signal

SFN System Frame Number

SNR Signal to Noise Ratio

SSS Secondary Synchronization Signal

UE User Equipment

WRx Wake-up Receiver

WUG Wake-up Group

WUID Unique Wake-up ID

WUS Wake-up Signal

List of Figures

List of Tables

Chapter 1

Introduction

Internet of Things (IoT) refers to the billions of devices which are capable of communicating with each other, either connected wirelessly or with physical wires. These devices communicate using different protocols. IoT devices are exponentially increasing in number, and are expected to be used in different areas of services like security, tracking and tracing, payment service, health-care, automatic control or remote-control, metering and consumer electronics.

Most IoT devices are battery powered and it is desirable that the energy in their batteries lasts longer. The capacity of a battery in an IoT device cannot be increased significantly due to the size constraints and it is an expensive choice. If not increasing the size, the batteries need to be replaced frequently and become a tedious job. Hence, we need to find energy efficient schemes to improve the longevity of these batteries. In order to do this, we need to scrutinize the present working principles of IoT devices in terms of their energy consumption. Apart from the operations handled by these devices, they consume a significant amount of the energy during the wireless communication [7]. During this wireless communication, one of the dominant components of energy cost is due to idle listening. To reduce this energy cost, the devices typically follow intermittent operation instead of a continuous operation. This technique is commonly known as duty cycling. Here, the device is active during the ON time, T_{ON}, and listens for potential communication. During the OFF time, T_{OFF}, or sleep time, the device is switched off and is unavailable for any communication. In such an intermittent operation scheme, both the amount of energy consumption and the device availability depends on the ON and OFF durations of the duty cycle.

The power consumption of a device varies when the receiver listening period is changed. Short and long duty cycles are shown in Figure 1.1, to illustrate the difference, with time on the horizontal axis and power consumption on the vertical axis. In Figure 1.1 (a), if the network wants to reach a device, which is following similar duty cycle, at time T, it waits for a shorter time interval to reach the device. At the same time instant, if the network wants to reach another device, which is following duty cycle similar to Figure 1.1 (b), it needs to wait for a much longer time compared to the earlier one. The main difference between these duty cycle configurations is the OFF time duration which results in better saving with longer cycles but the device becomes less available to the network. Hence, to save energy, devices should be configured with as long cycles as possible, while fulfilling the availability requirement.

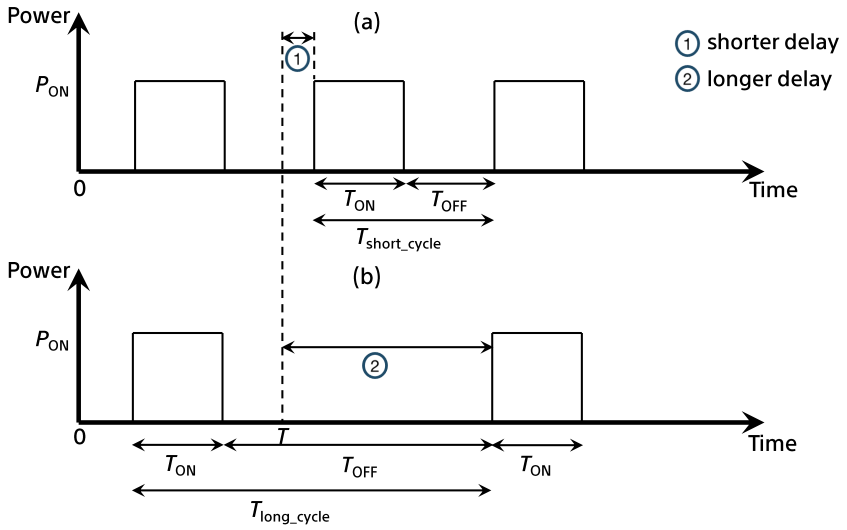

Figure 1.1: Illustration of two duty cycle configurations and its influence on delay (a) Short duty cycles (b) Long duty cycles

Based on the availability requirement, the IoT devices can be classified as delay tolerant or intolerant. For delay-intolerant devices, it is required that they are available with small delays for communication with the network and hence, configured with short duty cycles. The devices are made more available by increasing the idle listening period. This can sum up to a considerable energy waste. In this thesis, we analyze the energy saving schemes and investigate possible ways to reduce the idle channel listening energy cost. Our approach is to switch off the power-hungry Main Receiver (MRx) circuitry and use a Wake-up Receiver (WRx) to perform the duty cycling. Here, WRxs are capable of detecting the incoming transmission indicators and the power-hungry MRx circuitry switches on only when there is actual data transfer. The WRx concept is not new in the world of energy saving techniques but its integration in IoT devices connected to cellular networks is. In WSNs, with the introduction of WRxs, a considerable reduction in battery usage has been estimated [8] and [9]. In this thesis, the possibility of using WRx in the IoT devices within cellular networks is studied.

To analyze the energy consumption of IoT devices, we need to get familiar with the existing procedures for wireless communication in cellular networks.

1.1 Background

In cellular networks, IoT devices have to follow certain standard procedures for wireless communication. The Third Generation Partnership Project (3GPP) is responsible for the main telecommunication standards. They introduced Machine Type Communication (MTC) and Narrow-Band IoT (NB-IoT) concepts for communication among IoT devices without human intervention. The requirements for

these devices are typically set to low cost and low energy consumption. In this thesis, we focus on MTC working principles. The concept of duty cycling discussed earlier, is prevalent in cellular networks like Long Term Evolution (LTE) and LTE-Advanced (LTE-A), under the names, Discontinuous Transmission (DTX) and Discontinuous Reception (DRX) for transmission and reception, respectively in idle and connected mode, discussed later in this chapter. They were introduced in release 4 of the 3GPP standard and further modified as long and short DRX cycles in release 8. This enables the devices to leverage longer or shorter sleep duration to trade energy consumption for availability. DRX lets the receiver circuitry go to sleep mode as soon as the ON duration ends and remains OFF until the DRX cycle lasts. The sleep mode during the DRX cycle is referred to as light sleep where the device is set to go to sleep, even when the traffic queue is not completely empty. During this light sleep, the device radio stops listening to the channel while the remaining circuitry is still on, to maintain connectivity with the network. The power consumption during this light sleep is P_{ls}. Due to this intermediate power level P_{ls}, the device in DRX mode has shorter ON to OFF and OFF to ON transition times. A typical DRX cycle with ON and OFF duration is illustrated in Figure 1.2.

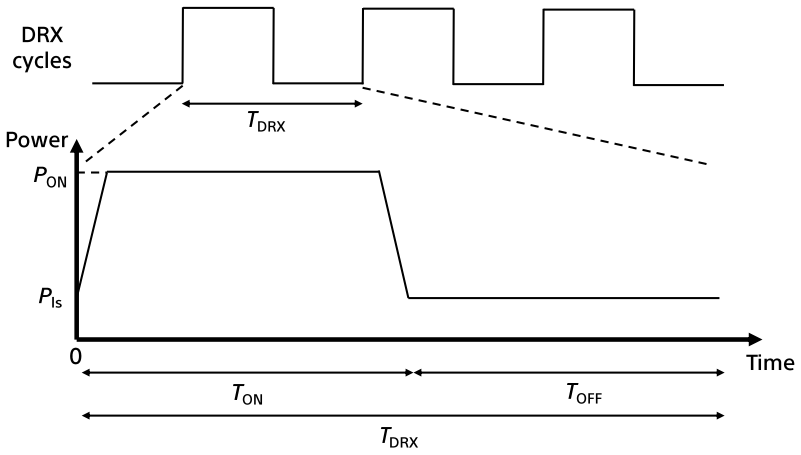

Figure 1.2: An individual DRX cycle with ON state power P_{ON}, OFF state or light sleep power P_{ls}, cycle time T_{DRX}, ON time T_{ON} and OFF time T_{OFF}

A device commonly referred to as User Equipment (UE), can duty cycle in two modes of operation, idle mode, and connected mode. In idle mode, it duty cycles to check if there is data or information update available for it. In connected mode, it duty cycles to ensure the end of an ongoing data transfer with the base station, hereafter referred to as eNodeB. Our focus in this thesis is the idle mode of operation, and we discuss the advantages of using a WRx in this mode. During the ON time in idle mode, a UE listens to the channel for a possible data transfer.

To initiate this data transfer, the eNodeB, transmit indicators before a data transfer and these indicators are known as paging indicators transmitted through the specific channel. The procedure of indicating a UE before data transfer is known as paging and the time instance of the paging is also known as a paging occasion in cellular networks. The paging procedure consists of a paging indication and a paging instruction in the form of a paging message. If the paging message is a call for data transfer, it moves on to the connected mode to communicate with the eNodeB, to proceed with data transfer, as shown in Figure 1.3.

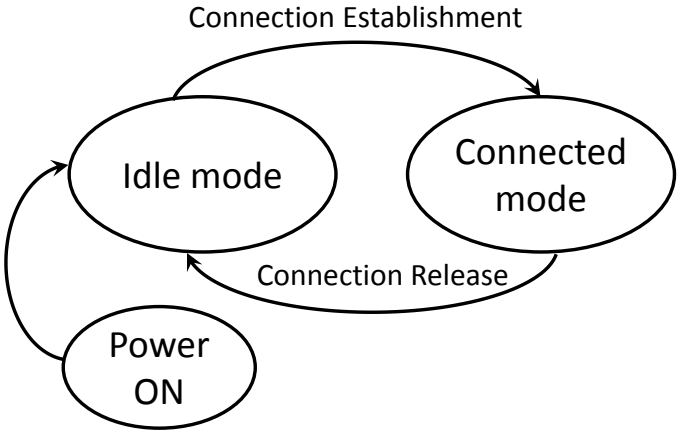

Figure 1.3: Idle and connected modes of operation of a UE

Using the DRX cycle configuration, the maximum cycle duration is limited to 2.56 s, sufficient for conventional mobile broadband requirements [6]. For the UEs with low availability requirement, using DRX cycle configuration results in a significant amount of idle-listening energy waste. To reduce the energy consumption of these UEs, 3GPP has introduced Power Saving Mode (PSM) in release 12. In PSM mode, the UE enters deep sleep, the state with near-zero power consumption, for a determined time interval. During this period, the UE cannot be reached by the eNodeB. Due to its inherent poor availability, PSM is best suited for UEs where the data transfer is initiated by the UE itself and network originating data is not delay critical. For UEs where data transfer is initiated by the network, and with low availability requirements, much longer duty cycles were introduced as extended DRX (eDRX) in release 13. This technique further reduces the energy consumption compared to DRX at the cost of UEs becoming less available for communication. During the ON state, the UE duty cycles for a duration termed Paging Time Window (PTW), to remain available intermittently for communication with the eNodeB. It has a longer ON state, giving enough room for the network to page the UE, increasing the availability of the UE. The energy saving of a UE operating with an eDRX cycle is more, compared to a UE operating with a DRX cycle due to its longer sleep time. A typical eDRX cycle is illustrated in

Figure 1.4 where the UE duty cycles within the PTW for a configured number of cycles. During this duty cycling, the UE goes to light sleep with a low power consumption P_{ls}, similar to the DRX cycle. After the PTW ends, it goes to deep sleep, with an even lower power consumption P_{ds}.

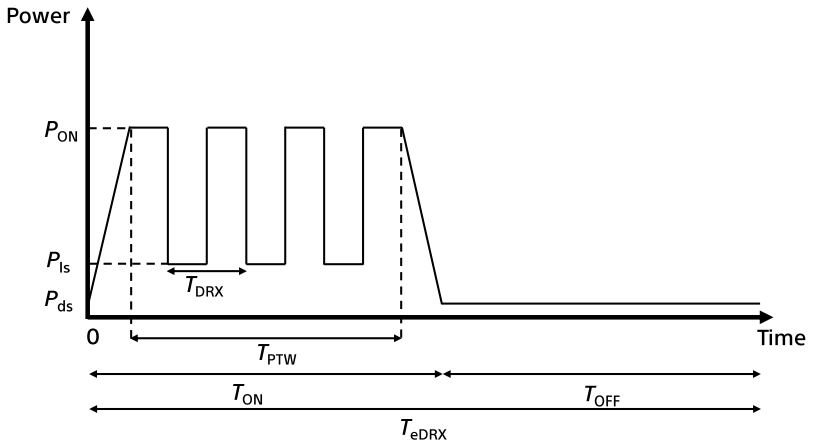

Figure 1.4: An eDRX cycle with ON state power P_{ON}, light sleep power P_{ls}, OFF state or deep sleep power P_{ds}, cycle time T_{edrx}, ON time T_{ON} and OFF time T_{OFF}

As discussed earlier, we analyze the performance of the receiver with and without an additional WRx in cellular networks. A cellular network is a synchronized system and therefore the time scheduling is important. To remain available to communicate with the eNodeB, the UE needs to wake up at a specific time instant. For that, remaining synchronized with the eNodeB clock, expressed in terms of radio frames, is vital. The communication between the eNodeB and the UE is possible when their respective clocks match each other. In LTE, the clock is represented by the System Frame Number (SFN) and the sub-frame numbers. In order to provide timing reference for the UEs, the eNodeB transmits a Primary Synchronization Signal (PSS) and a Secondary Synchronization Signal (SSS) [6]. Once a UE reads these signals, it is said to be radio frame synchronized with the eNodeB. For simplicity, this radio frame synchronization is hereafter referred to as sync. When a UE sleeps for a longer period, it loses its synchronization with the eNodeB and it has to regain this sync when it wakes up. This is costly in terms of energy consumption and becomes even costlier if the UE is positioned in a bad coverage area. Moreover, the UE during its sleep time experiences a clock drift in both time and frequency domains, relative to the clock of the eNodeB, this needs to be taken care of and is estimated in our thesis. The decoding time for the sync signals and channel information is dependent on the distance of the UE from the eNodeB. Based on the received Signal to Noise Ratio (SNR) at the UE, the signals from the eNodeB need to be sent repeatedly so that the UE can build up the SNR

to a required level by combining multiple copies of the signal. To reduce the UE energy consumption during the idle mode, a Wake-up Signal (WUS) is introduced in 3GPP release 15 [2]. A WUS is an indication sent to a particular UE or a group of UEs, to start reading the respective channels for a paging. The UEs continue to read further only when the correct WUS is sent by the eNodeB. In this way, it saves the energy required to read the channels unnecessarily in order to remain available for communication. To facilitate easier and faster sync, a new sync signal is introduced in release 15, which can be acquired in a shorter time compared to the previous sync signal [3]. This new sync signal is called as a Resynchronization Signal (RSS).

In this thesis, we continue to investigate further, with the introduction of WRx, to what extent energy can be saved. We analyze and infer if it is possible to suffice the future needs using the same battery or if it is robust and efficient enough to reduce the battery size even further. The WUS is received by WRx as a confirmation to trigger MRx to start reading the channel information. Hence, the WRx should be capable of receiving the WUS and this also leads us to the design of suitable WUS for WRx.

1.2 Outline

After this introduction, Chapter 2 presents the approach and methodology of the project. In Chapter 3, the energy consumption and delays for the existing techniques, and introduction of WRx which is the solution we investigate, are described. Chapter 4 discusses the WRx, WUS designs and their corresponding processing units. It also presents the simulation results of different WUS designs, analyses them and proposes effective WRx characteristics and a WUS design. Based on this design, in Chapter 5, power, and delays in SoA techniques and our investigated solution are analyzed. Power consumption with the introduction of WRx is compared to those of SoA solutions and the respective power savings are calculated. Chapter 6 gives the conclusion and presents ideas for future work.

Chapter 2
Approach and Methodology

As described in the introduction, our intention in this thesis work is to minimize the energy consumed by the UEs in cellular networks. In this chapter, we describe our approach and methods for reducing the energy consumption of the UEs and how we proceed further in our investigation.

2.1 Approach

Our approach to reduce the energy consumption is to investigate how low-power WRxs can be used to save energy and enhance the battery life of a UE. The main purpose of having a WRx in the receiver circuitry is to perform the duty cycling on behalf of MRx at a lower power consumption and as soon as it receives WUS, it wakes up the MRx to perform its normal operation. The low power consumption of WRxs allows the UEs to be active for longer periods than the SoA techniques, monitoring the channel for communication, using the same amount of energy as it would consume using MRx for a much shorter period. It is worthwhile to mention that this power saving comes along with a performance loss due to the WRx design [8]. The low power receiver has a higher noise figure which degrades the performance of the receiver compared to the MRx. This performance loss can be interpreted in terms of bit-error rate of the received signal which influences the detection of WUS by WRx. Hence, the design of new WUS is of importance. Improper WUS design can lead to false alarms where noise is detected as WUS and also increase energy loss due to waking up after receiving WUSs intended for the neighbouring UEs. This phenomenon is known as overhearing. The new WUS is designed to avoid such false triggers and to reduce the overhearing energy cost.

2.2 Methodology

In our investigation to reduce energy consumption, the methodology we choose is a combination of WUS performance simulations and analytic energy consumption calculations. Using the probabilities of detection and false alarm, achieved from the performance simulations, we calculate the energy consumption and delays using analytical expressions. These analytical expressions are derived on the basis of state diagrams of the UEs operations during the idle mode operation for the existing solutions and the investigated case in DRX and eDRX modes.

Next, we compare our investigated solution with the existing solutions and evaluate the relative power saving. This helps us in proposing a final solution with a good trade-off between energy consumption and the UE availability.

Chapter 3

Power Consumption and Delay Calculations

In this chapter, we calculate the power consumption and delay in reaching the UE, by deriving the equations for the UE's energy consumption for the existing schemes and our investigated solution. To derive these equations, we follow the state diagrams for each scheme. The state diagrams follow the path governed by respective probabilities. To do this, we need to understand the operational states in each power saving scheme.

To start with, let us first get acquainted with the existing schemes and the investigated solution before moving into energy and delay calculations. We have considered two existing schemes as our reference to analyze our investigated solution. Now, we describe briefly our considered cases.

Reference cases: We consider two existing schemes. The first scheme is selected to be the one where during the idle mode of operation of a UE, there is no WUS. The UE reads only a paging indicator to continue reading the paging message. The second scheme includes a WUS in the idle mode of operation where the UE first detects WUS before checking for any paging indicator. We term the schemes as No-WUS and MWUS respectively. The MWUS scheme is a better solution than the No-WUS scheme in terms of energy consumption. With the introduction of WUS in MWUS scheme, it reduces the energy cost of idle channel listening and to some extent the overhearing energy cost. This shortens the idle channel listening cost by the receiver. We compare the investigated solution with the reference cases and evaluate the amount of energy saving achieved over the two distinct cases.

Investigated solution: Our investigated solution is the usage of WRx along with the existing receiver. During the idle mode of operation, WRx duty cycles in place of MRx to receive the WUS. The WRx is a low power non-coherent receiver. In this thesis, we investigate if the integration of such a receiver within the UE helps to enhance energy saving. Even WRx needs a WUS to trigger the MRx for further operations but in order to save energy, a new efficient WUS has to be designed. This combination of WRx and new WUS is referred to as WWUS case. With the introduction of WRx, we investigate the power consumption in both DRX and eDRX modes of operation, with the aim to further reduce the idle listening, overhearing and false alarm costs. Similar to the MWUS case, the WUS

is assumed to be scheduled ahead of the paging occasion, before the MRx starts duty cycling. In the earlier case, the MRx duty cycles to receive the WUS but in the investigated solution, the same duty cycling is done by WRx at much lower power consumption.

To understand the UE operations in both the reference cases and the solution we investigate, we follow the state diagrams. Each operational state in the state diagrams represents the action it performs and also includes information regarding the corresponding power (P) and time (T) spent to perform that operation. In case of repetitions involved to complete the reading process, the number of repetitions (R) is also mentioned in the respective operational state(s). The product of the power, time and number of repetitions if involved, give us the energy cost in that particular operational state. The branching of the path in the state diagram is governed by respective probabilities. These probabilities vary from case to case and will be defined when we come across them.

Another important aspect which we focus in this thesis is the time it takes for eNodeB to reach the UE. Hence, the delay to approach a UE needs to be calculated along with the average power consumption. In the next section, we first see how the expressions for the UE energy consumption within a cycle are derived following their respective state diagrams. Next, we formulate the average delay to reach a UE in both power saving modes of operation, DRX, and eDRX, for all the considered cases.

3.1 Reference Cases: DRX Power Consumption and Delay Calculations

A DRX cycle is a short period in which a UE switches on and off and repeats the cycles to remain available to the eNodeB. In this section, we calculate the average power consumption in one DRX cycle and later the delay before eNodeB can reach the UE, for the reference cases, i.e., No-WUS and MWUS. The variables used in each operational state are introduced in the respective state diagrams and the expressions to calculate the energy consumption and delay are presented.

3.1.1 No-WUS: Power Consumption

For No-WUS case, in idle mode, the UE performs the activities as shown in Figure 3.1 and we derive the average power consumption following the corresponding operational state energy costs as shown in the state diagram. The average power consumption is given by

$$P_{\text{avg}}^{\text{drx}} = \frac{E_{\text{No-WUS}}^{\text{drx}}}{T^{\text{drx}}}, \tag{3.1}$$

where, T^{drx} is the configured DRX cycle time and E^{drx} is the average energy consumption, derived by summing up the energy costs in the operational states. To find the UE energy consumption, we need to understand the concept behind the different states included in the state diagram.

In all the DRX cycles, a UE performs similar activities as shown in Figure 3.1 during the idle mode of operation. As we have discussed earlier, the sleep time

increases the power saving but it has an adverse effect on the clock drift of UEs. With the sleep time, the clock of a UE drifts from the eNodeB clock. During its normal operation, a UE first ramps up to its ON state according to an estimated time drift of clock. This time advancement enables the UE to match its clock with eNodeB. In the No-WUS case, a UE reads the Machine Type Communication Physical Downlink Control Channel (MPDCCH) to check for the presence of a paging indication called Paging-Radio Network Temporary Identifier (P-RNTI). If there is a P-RNTI, the UE continues to read the paging message in the Physical Downlink Shared Control Channel (PDSCH) to check if the data is intended for that particular UE. A paging message contains the identities of the UEs being paged. If the UE finds its identity in the paging message, it switches to the connected mode to read the Physical Random Access Channel (PRACH), which is beyond the scope of this thesis. If the UE does not detect a P-RNTI in MPDCCH or does not find its identity in the paging message, then it moves to sleep state. There is a possibility of error event due to detection of noise as P-RNTI or reading other indications to be a P-RNTI. This event is known as a false alarm. We must remember that we are discussing a synchronous network and the eNodeB schedules the paging based on the traffic. The UE cycle time is configured accordingly well in advance, so that eNodeB can communicate with the UE during the ON duration of a DRX cycle.

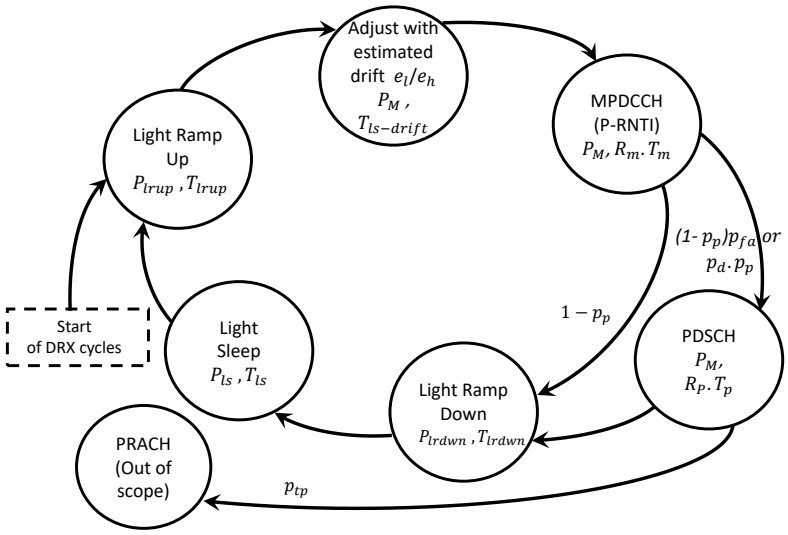

Figure 3.1: State diagram for DRX cycling (No-WUS case)

Before discussing the energy consumption for the No-WUS case, we need to make an assumption. Due to the short periods of DRX cycles, the UEs are very unlikely to lose their sync. Hence, we do not consider any sync time for DRX mode average power calculation. Now, if we sum up the energy costs of the operational states with the aim to achieve the average energy cost during a DRX cycle including all possible branching, we arrive at (3.2). The branches as discussed earlier are

governed by probabilities, and we specify each of them following the equation,

$$\begin{aligned} E^{\text{drx}}_{\text{No-WUS}} =& P_{\text{lrup}} T_{\text{lrup}} + P_{\text{M}} T_{\text{ls-drift}} + P_{\text{M}} T_{\text{m}} R_{\text{m}} \\ &+ \left[p_{\text{p}} \cdot p_{\text{d}} + (1 - p_{\text{p}}) p_{\text{fa}}\right] P_{\text{M}} (T_{\text{prt}} + T_{\text{p}} R_{\text{p}}) \\ &+ P_{\text{lrdwn}} T_{\text{lrdwn}} + P_{\text{ls}} T^{\text{drx}}_{\text{ls}} \end{aligned} \tag{3.2}$$

where, each line represents different energy costs, contributing to the total average energy consumption, and we discuss them below, one by one. The first line represents the light ramp up energy cost, the energy cost associated with the estimated time drift due to previous cycle light sleep time, and the idle listening energy cost where R_{m} is the number of MPDCCH repetitions. The second line gives the energy cost for reading PDSCH during a page, governed by probability of paging p_{p} and probability of detection p_{d}, and the energy cost due to error in detection or false alarm when there is no paging is governed by probability of no paging and probability of false alarm p_{fa}. Finally, the third line gives the light ramp down energy cost and the sleep time energy cost. The sleep time energy cost calculation is provided in Appendix, section A.1 for reference.

Now that we understood the way we derive the energy equation, by replacing (3.2) in (3.1) for a chosen DRX cycle time, we get the corresponding average power consumption, P^{drx}. Now we continue to derive the same for MWUS case.

3.1.2 MWUS: Power Consumption

In MWUS case, the calculation of power consumption is similar to the No-WUS case. Here, the energy cost of idle listening gets reduced and it is reflected in the state diagram as shown in Figure 3.2. If we investigate the operational states involved in the MWUS case, we find an additional WUS operational state. Earlier, for the No-WUS reference case, average power consumption is calculated without considering the WUS operational state. With the introduction of WUS, the UE first listens for a WUS. Only on a detection of a correct WUS, it continues to read the MPDCCH and thereby, the cost of unnecessary reading of MPDCCH which gets multiplied with the repetitions is reduced. To find the UE average energy cost in a configured DRX cycle, similar to the No-WUS case, we aggregate the energy cost in each operational state along with its branches.

Within a DRX cycle, after ramping up to ON state and adjusting the clock by using an estimated drift time, the UE listens to the channel for a WUS. A WUS can either be for a target group of UEs or a non-target group of UEs. A UE only on detecting the correct WUS moves on to read MPDCCH. Within a wake-up group, the number of UEs is dependent on the WUS design. In this case, based on the target group, the target and non-target UEs cannot be segregated. A UE within a target group can validate if there is a data available for itself, only after reading the PDSCH. Hence, equal energy costs are involved for a target UE and a non-target UE within a target group WUS. In case the UE receives a non-target group WUS or do not receive a WUS, the UE energy cost during the DRX cycle is limited to WUS reading. In case of false alarm where a UE detects noise or a non-target WUS as a target WUS, the UE proceeds to read MPDCCH which is unavoidable.

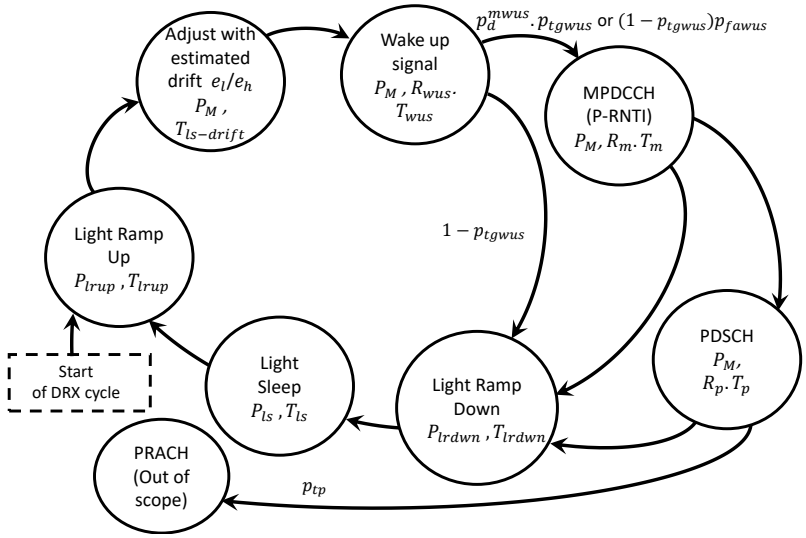

Figure 3.2: State diagram for DRX cycling with WUS received by MRx

Now to formulate the average energy consumption $E_{\mathrm{MWUS}}^{\mathrm{drx}}$, we use a similar technique to No-WUS case and find the following expression,

$$\begin{aligned} E_{\mathrm{MWUS}}^{\mathrm{drx}} =& P_{\mathrm{lrup}} T_{\mathrm{lrup}} + P_{\mathrm{M}} T_{\text{ls-drift}} + P_{\mathrm{M}} T_{\mathrm{wus}} R_{\mathrm{wus}} \\ &+ p_{\mathrm{tgwus}} \cdot p_{\mathrm{d}}^{\mathrm{mwus}} \cdot P_{\mathrm{M}} (T_{\mathrm{m}} R_{\mathrm{m}} + T_{\mathrm{prt}} + T_{\mathrm{p}} R_{\mathrm{p}}) \\ &+ (1 - p_{\mathrm{tgwus}}) p_{\mathrm{fa}} \cdot P_{\mathrm{M}} (T_{\mathrm{m}} R_{\mathrm{m}}) \\ &+ P_{\mathrm{lrdwn}} T_{\mathrm{lrdwn}} + P_{\mathrm{ls}} T_{\mathrm{ls}}^{\mathrm{drx}} \end{aligned} \tag{3.3}$$

where, each line represents the contribution of different energy cost bearers which constitutes the total average energy. The first line of the equation represents the energy cost to ramp up, adjust drift and read the WUS. The second line gives the energy cost to read the MPDCCH and PDSCH in case of correct detection of the target group WUS where p_{tgwus} is the probability of occurrence of a target group WUS and $p_{\mathrm{d}}^{\mathrm{mwus}}$ is the probability of detection of the WUS by MRx. The third line represents the energy cost to read MPDCCH in case of a false alarm and finally, the fourth line gives the energy cost to ramp down and sleep.

Now that we have the power consumption expressions for the reference cases in DRX cycle, we continue to find the delay calculation expressions.

3.1.3 DRX Delay Calculations

The time delay to reach a UE by the eNodeB is another parameter we consider along with the power consumption to evaluate the energy saving schemes. We assume that the eNodeB is equally likely to have data available for a UE at any random time instant during the UE's sleep time. Hence, the average minimum delay in reaching the UE is half of the UE sleep time, $\frac{T_{\mathrm{ls}}^{\mathrm{drx}}}{2}$. Depending on the

probabilities of detection p_{d} and miss $(1-p_{\mathrm{d}})$, the delay can further increase by a cycle time if the UE misses or does not detect the page for No-WUS case or misses the WUS for MWUS case. Considering these probabilities and solving the infinite series, we derive the delay expressions. The delay (D) to reach a UE by the eNodeB depends on the probability of detecting the WUS correctly and with each miss, the eNodeB has to wait for another cycle time to reach the UE. To calculate this probability, we need to consider a sum of infinite arithmetic-geometric series. The expression for average delay including the series is given by,

$$\begin{aligned} D^{\mathrm{drx}} &= \frac{T_{\mathrm{ls}}^{\mathrm{drx}}}{2} + T_{\mathrm{lrup}} + T_{\text{ls-drift}} + T_{\mathrm{m}}R_{\mathrm{m}} + T_{\mathrm{prt}} + T_{\mathrm{p}}R_{\mathrm{p}} \\ &\quad + p_{\mathrm{d}}(1-p_{\mathrm{d}})T^{\mathrm{drx}} + 2p_{\mathrm{d}}(1-p_{\mathrm{d}})^2T^{\mathrm{drx}} + ... \\ &= \frac{T_{\mathrm{ls}}^{\mathrm{drx}}}{2} + T_{\mathrm{lrup}} + T_{\text{ls-drift}} + T_{\mathrm{m}}R_{\mathrm{m}} + T_{\mathrm{prt}} + T_{\mathrm{p}}R_{\mathrm{p}} \\ &\quad + p_{\mathrm{d}}(1-p_{\mathrm{d}})T^{\mathrm{drx}}\Big[1 + 2(1-p_{\mathrm{d}}) + 3(1-p_{\mathrm{d}})^2 + ...\Big] \end{aligned} \tag{3.4}$$

In (3.4), the first line refers to the minimum delay to reach the UE, which happens in case of no errors. The second line refers to the delay in case of errors and it is an arithmetic-geometric series which evaluates to $\left(\frac{1-p_{\mathrm{d}}}{p_{\mathrm{d}}}\right)$.

Here, we present the expressions for the delay before eNodeB can reach the UE, for the reference cases.

No-WUS case: The average delay to detect a paging for the No-WUS case is given by

$$D_{\text{No-WUS}}^{\mathrm{drx}} = \frac{T_{\mathrm{ls}}^{\mathrm{drx}}}{2} + T_{\mathrm{lrup}} + T_{\text{ls-drift}} + T_{\mathrm{m}}R_{\mathrm{m}} + T_{\mathrm{prt}} + T_{\mathrm{p}}R_{\mathrm{p}} + \left(\frac{1-p_{\mathrm{d}}}{p_{\mathrm{d}}}\right)T^{\mathrm{drx}}. \tag{3.5}$$

MWUS case: With the MWUS case, the average delay to detect a page includes the time to detect WUS and paging. In case of unsuccessful detection of WUS, the delay increased by a cycle time and the probability is calculated using a similar technique followed in No-WUS case. The average delay to detect a paging for MWUS case is expressed as

$$\begin{aligned} D_{\mathrm{MWUS}}^{\mathrm{drx}} = &\frac{T_{\mathrm{ls}}^{\mathrm{drx}}}{2} + T_{\mathrm{lrup}} + T_{\text{ls-drift}} + R_{\mathrm{wus}}T_{\mathrm{wus}} + T_{\mathrm{m}}R_{\mathrm{m}} + T_{\mathrm{prt}} + T_{\mathrm{p}}R_{\mathrm{p}} \\ &+ \left(\frac{1-p_{\mathrm{d}}^{\mathrm{mwus}}}{p_{\mathrm{d}}^{\mathrm{mwus}}}\right)T^{\mathrm{drx}}. \end{aligned} \tag{3.6}$$

Now, that we have the power consumption and delay expressions for the reference cases in DRX cycle, we continue to find the average power consumption and delay for our investigated solution in the next section.

3.2 WWUS: DRX Power Consumption and Delay Calculation

In this section, we derive the power and delay expressions for the investigated solution. Here, both MRx and WRx are taken into consideration and the corre-

sponding operational states are described. The total energy cost is given as an aggregate of the energies consumed by MRx and WRx based on the UE operations.

3.2.1 WWUS: Power Consumption

In our investigated solution, WWUS, we have similar operational states like reference cases but with the inclusion of WRx dedicated for WUS, it results in a slight change in its state diagram shown in Figure 3.3 compared to Figure 3.2. Another difference in energy cost is the lower power consumption of WRx. In this case, a WRx is used to receive a WUS and switches on of the MRx circuitry commences on a successful reception of WUS by WRx. While the WRx listens for the WUS, MRx is in a deep sleep state. Hence, re-synchronization with the network is required, resulting in additional energy cost when the MRx wakes up. After receiving a trigger from WRx, the MRx ramps up and adjusts the clock according to the estimated drift, and synchronizes with enodeB clock. Once the sync is acquired, the MRx starts its usual MPDCCH reading to find P-RNTI. Then the UE continues to read PDSCH to check for its UE identity to confirm if there is data available for it. In case of non-target group WUS and no WUS received, the WRx goes back to deep sleep and does not trigger the MRx to switch on. When a UE detects noise or WUS for other UE groups as its own WUS, the WRx triggers the MRx and the associated cost with this event is unavoidable.

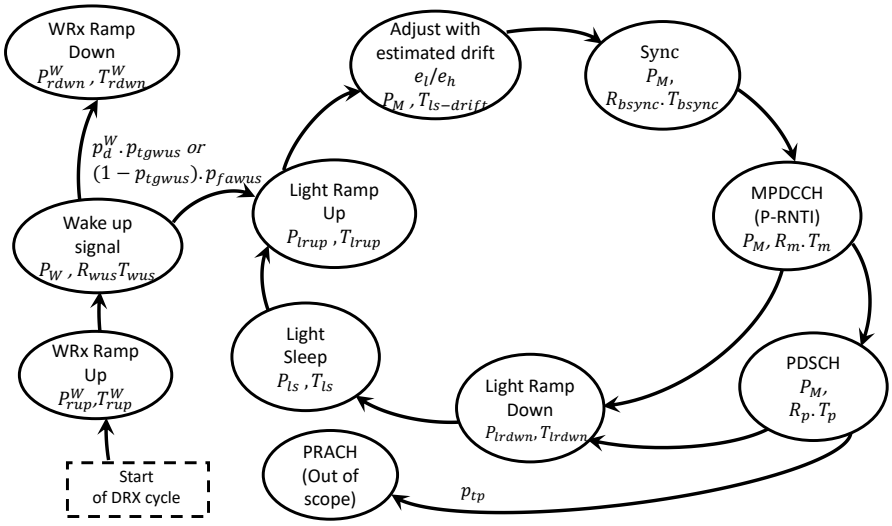

Figure 3.3: State diagram for DRX cycling with WUS received by WRx

As discussed in chapter 1, in release 15, 3GPP has brought in a new sync signal. We denote the time to read the re-sync signal as T_{bsync} and the repetitions as R_{bsync} in our average power consumption calculation. The operational state sync will take place depending on the sleep duration of the MRx. This operational state is optional for DRX cycle energy calculation but it is included in the average

energy calculation in our consideration. The average energy consumption of a UE in WWUS case includes the energy costs of both the WRx and MRx. A fixed energy cost is contributed by the WRx in every duty cycle and this energy consumed by the WRx is given by, $E^{\mathrm{W}}_{\mathrm{wus}}$ is given by

$$E^{\mathrm{W}}_{\mathrm{wus}} = P^{\mathrm{W}}_{\mathrm{rup}} T^{\mathrm{W}}_{\mathrm{rup}} + P_{\mathrm{W}} T^{\mathrm{W}}_{\mathrm{drift}} + P_{\mathrm{W}} T^{\mathrm{W}}_{\mathrm{wus}} R^{\mathrm{W}}_{\mathrm{wus}} + P^{\mathrm{W}}_{\mathrm{rdwn}} T^{\mathrm{W}}_{\mathrm{rdwn}}, \tag{3.7}$$

where, $P^{\mathrm{W}}_{\mathrm{rup}} T^{\mathrm{W}}_{\mathrm{rup}}$ is the ramp up energy cost of WRx, $P_{\mathrm{W}} T^{\mathrm{W}}_{\mathrm{drift}}$ is the energy cost associated with the drift time estimation of WRx, $P_{\mathrm{W}} R^{\mathrm{W}}_{\mathrm{wus}} T^{\mathrm{W}}_{\mathrm{wus}}$ is the energy cost to read the WUS by WRx and $P^{\mathrm{W}}_{\mathrm{rdwn}} T^{\mathrm{W}}_{\mathrm{rdwn}}$ is the energy cost of ramp down energy cost of WRx.

The total average energy consumption of a UE in DRX mode in WWUS case including the energy costs of MRx and WRx, $E^{\mathrm{drx}}_{\mathrm{WWUS}}$ is given by

$$\begin{aligned} E^{\mathrm{drx}}_{\mathrm{WWUS}} =& E^{\mathrm{W}}_{\mathrm{wus}} + p_{\mathrm{tgwus}} \cdot p^{\mathrm{W}}_{\mathrm{d}} \Big[P_{\mathrm{drup}} T_{\mathrm{drup}} + P_{\mathrm{M}} (T_{\text{ds-drift}} \\ & + T_{\mathrm{bsync}} R_{\mathrm{bsync}} + T_{\mathrm{m}} R_{\mathrm{m}} + T_{\mathrm{prt}} + T_{\mathrm{p}} R_{\mathrm{p}}) + P_{\mathrm{drdwn}} T_{\mathrm{drdwn}} \Big] \\ & + (1 - p_{\mathrm{tgwus}}) p^{\mathrm{W}}_{\mathrm{fawus}} \Big[P_{\mathrm{drup}} T_{\mathrm{drup}} + P_{\mathrm{M}} (T_{\text{ds-drift}} \\ & + T_{\mathrm{bsync}} R_{\mathrm{bsync}} + T_{\mathrm{m}} R_{\mathrm{m}}) + P_{\mathrm{drdwn}} T_{\mathrm{drdwn}} \Big] \\ & + P_{\mathrm{ds}} T^{\mathrm{drx}}_{\mathrm{ds}}, \end{aligned} \tag{3.8}$$

where each line represents different energy contributions. $p_{\mathrm{tgwus}} \cdot p^{\mathrm{W}}_{\mathrm{d}}$ is the probability with which the WRx triggers the MRx, on reception of the WUS with probability p_{tgwus} and detecting it with the probability $p^{\mathrm{W}}_{\mathrm{d}}$. $(1 - p_{\mathrm{tgwus}}) p_{\mathrm{fawus}}$ is the probability with which WRx triggers the MRx in case of noise or non-target WUS detected as the expected WUS where p_{fawus} is the probability of false alarm. $P_{\mathrm{ds}} T^{\mathrm{drx}}_{\mathrm{ds}}$ is the energy cost during the deep sleep time. The term e_{rtc} is the correction factor used to estimate the drift time caused by deep sleep and the estimation calculations are described in the last section of this chapter.

3.2.2 WWUS: Delay Calculation

For the delay in WWUS case, we derive the expression in a similar way like reference cases. The average minimum delay for reaching the device is half of previous cycle sleep time given by $\frac{T^{\mathrm{drx}}_{\mathrm{ds}}}{2}$. Together with the time for detecting the WUS and paging, delay is calculated in a similar method deriving arithmetic-geometric progression for probability of misses before correct detection like reference cases. For WWUS case, the average delay is given by sum of above mentioned delay components,

$$\begin{aligned} D^{\mathrm{drx}}_{\mathrm{WWUS}} =& \frac{T^{\mathrm{drx}}_{\mathrm{ds}}}{2} + T^{\mathrm{W}}_{\mathrm{rup}} + T^{\mathrm{W}}_{\mathrm{drift}} + R^{\mathrm{W}}_{\mathrm{wus}} T^{\mathrm{W}}_{\mathrm{wus}} + T^{\mathrm{W}}_{\mathrm{rdwn}} + T_{\mathrm{switch}} + T_{\mathrm{drup}} \\ & + T_{\text{ds-drift}} + T_{\mathrm{bsync}} R_{\mathrm{bsync}} + T_{\mathrm{m}} R_{\mathrm{m}} + T_{\mathrm{prt}} + T_{\mathrm{p}} R_{\mathrm{p}} \\ & + \left(\frac{1 - p^{\mathrm{W}}_{\mathrm{d}}}{p^{\mathrm{W}}_{\mathrm{d}}} \right) T^{\mathrm{drx}} \end{aligned} \tag{3.9}$$

If we consider UEs configured to DRX mode of operation, there can be challenges in real life implementation of the WWUS solution. The WRx listens to the WUS ahead of the paging time, so that it can trigger the MRx in time. In case of very short DRX cycles, it is unlikely that the WRx listens to the WUS and immediately wakes up the MRx. The switching time from WRx to MRx can be higher than the DRX cycle time chosen, depending on the WRx design. Hence, it may not be the ideal solution for those UEs. But WRx can still be used for idle listening if a larger time gap between the WUS instance and the paging occasion is configured. For UEs configured to very short DRX cycle operation and require short time gap after WUS detection, following the MWUS mode of operation is more logical.

Now that we have the details about working of DRX, average energy consumption and delay calculations for the reference cases and investigated solution, we continue to derive the same in case of UEs configured with eDRX cycles.

3.3 Reference Cases: eDRX Power Consumption and Delay Calculations

An eDRX cycle has much longer cycle time compared to a DRX cycle. As discussed earlier, the UE following eDRX configuration, duty cycles during its ON time to remain available to the eNodeB for a longer period. The sleep duration during an eDRX cycle is also much longer compared to a DRX cycle, which leads to more power saving. In this section, we calculate the average power consumption and the delay to reach the UE, for the reference cases, No-WUS and MWUS in eDRX mode of operation. Similar to the description of UE operation in DRX mode, the operational states followed by the UE in eDRX mode, for the reference cases are described with the help of respective state diagrams. To derive the expressions to calculate the energy consumption, we adapt a similar way as shown in previous sections.

3.3.1 No-WUS: Power Consumption

To calculate the power consumption of a UE in eDRX mode of operation, we repeat the derivations following the state diagram in Figure 3.4. The energy calculation differs from DRX cycle since the sleep time power consumption is lower compared to that of DRX cycle as discussed in Chapter 1. According to the state diagram, the UE ramps up to the ON state from deep sleep state, adjusts its clock with an estimated drift and synchronizes with the eNodeB to read MPDCCH. Here, the synchronization is an additional cost in this mode as the UE during its previous cycle deep sleep time, it is likely to lose its sync with the eNodeB's clock. As discussed before, in an eDRX cycle, during the ON time referred to as PTW, the UE duty cycles for a configured number of DRX cycles. In each duty cycle within the PTW, the UE looks for a P-RNTI in MPDCCH and continues to the next operational states, following the same logic as mentioned in No-WUS case in DRX cycle. The same procedures are followed in all the DRX cycles within the PTW. When a UE detects P-RNTI in MPDCCH and finds its identity in the PDSCH,

then it continues to read the PRACH and enters the connected mode of operation. In case of a false alarm, similar to the DRX mode of operation, the UE continues to read the PDSCH resulting in additional energy cost.

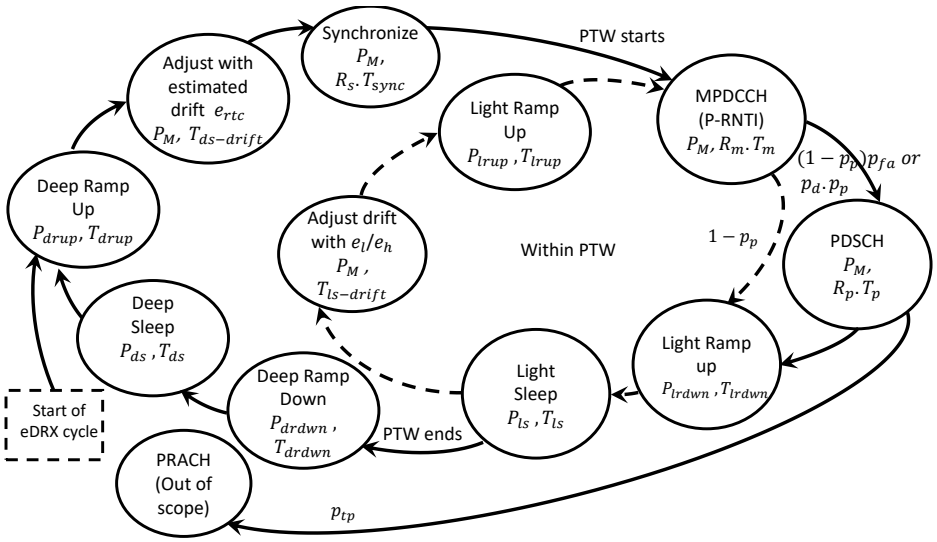

Figure 3.4: State Diagram for eDRX cycling (No-WUS case)

In the eDRX mode of operation, the number of DRX cycles in the PTW is chosen such that the eNodeB has enough time to reach the UE. Within the PTW, the eNodeB schedules the paging message dynamically and there is no particular distribution for the availability of a paging message. If the eNodeB wants to page a UE following eDRX configuration, once the UE wakes up, it sends the paging message as early as possible based on the network traffic. It is more likely that the UE finds the paging message in the first DRX cycle within the PTW. The probability of UE being paged in the subsequent DRX cycles decreases following a decaying progression. Therefore, let us assume that the probability of UE finding a paging message within a PTW, follows a geometric distribution with a decay coefficient α. With this assumption and in presence of a paging message, the probability of finding a page in i^{th} DRX cycle in a PTW can be expressed as

$$p(i) = \frac{1-\alpha}{1-\alpha^n} \cdot \alpha^{i-1}, \tag{3.10}$$

where, n is the configured number of DRX cycles in a PTW and α is the geometric decay constant. As we consider UE operation in idle mode, we calculate the energy consumed by the UE until it finds a paging message and assume that the UE enters deep sleep mode for the rest of the cycle. In the absence of a paging message, the UE performs idle listening for the scheduled number of DRX cycles and goes back to sleep. Similar to the DRX cycle operation, we include the possibility of an error occurrence in case of bad channel conditions or bad receiver operational characteristics, if the UE falsely detects noise as P-RNTI, it continues to read the PDSCH unnecessarily. Now that we understand, the UE operation in the eDRX

mode, the average energy consumed by the UE for the No-WUS case in an eDRX cycle is given by

$$
\begin{aligned}
E^{\text{edrx}}_{\text{No-WUS}} =& P_{\text{drup}} T_{\text{drup}} + P_{\text{M}} T_{\text{ds-drift}} + P_{\text{M}} T_{\text{sync}} R_{\text{sync}} \\
&+ (1 - p_{\text{p}}) n (P_{\text{lrup}} T_{\text{lrup}} + P_{\text{M}} T_{\text{ls-drift}} + P_{\text{M}} T_{\text{m}} R_{\text{m}} + P_{\text{lrdwn}} T_{\text{lrdwn}}) \\
&+ p_{\text{tp}} \Bigg[\sum_{i=1}^{n} p(i) \big[i (P_{\text{lrup}} T_{\text{lrup}} + P_{\text{M}} T_{\text{ls-drift}} + P_{\text{M}} T_{\text{m}} R_{\text{m}} + P_{\text{lrdwn}} T_{\text{lrdwn}}) \\
&+ P_{\text{M}} (T_{\text{prt}} + T_{\text{p}} R_{\text{p}}) \big] \Bigg] \\
&+ p_{\text{ntp}} \Big[n (P_{\text{lrup}} T_{\text{lrup}} + P_{\text{M}} T_{\text{ls-drift}} + P_{\text{M}} T_{\text{m}} R_{\text{m}} + P_{\text{lrdwn}} T_{\text{lrdwn}}) \\
&+ p_{\text{d}} \cdot P_{\text{M}} (T_{\text{prt}} + T_{\text{p}} R_{\text{p}}) \Big] \\
&+ (1 - p_{\text{p}}) p_{\text{fa}} \big[n P_{\text{M}} (T_{\text{prt}} + T_{\text{p}} R_{\text{p}}) \big] \\
&+ P_{\text{ls}} T^{\text{edrx}}_{\text{ls}} + P_{\text{drdwn}} T_{\text{drdwn}} + P_{\text{ds}} T^{\text{edrx}}_{\text{ds}} \\
&- P_{\text{M}} (T_{\text{ls-drift}} + P_{\text{lrup}} T_{\text{lrup}} + P_{\text{lrdwn}} T_{\text{lrdwn}}),
\end{aligned}
\tag{3.11}
$$

where, each line represent energy contribution of different events. The first term is the energy cost for ramping up from deep sleep state directly to the ON state, the second term is the additional energy cost spent in waking up earlier from deep sleep, and the third term in the first line of the equation is the energy cost required for the UE to acquire synchronization with the eNodeB. The second line represents the idle listening energy cost governed the probability of not finding a page $(1 - p_{\text{p}})$. The third and fourth line gives the energy cost when a target paging occurs with the probability p_{tp} and $p(i)$ is the probability of paging in the i_{th} DRX cycle as expressed in (3.10). The fifth and sixth line represent the energy cost when there is a paging for other devices in the cell with the probability p_{ntp}. The seventh line gives the additional energy cost in case of an error event when there is no paging with the probability $(1 - p_{\text{p}})$ and probability of false alarm p_{fa}. In the eighth line, the first term is the energy cost during the light sleep period within the PTW, second term is the energy cost for ramping down from ON state directly to the deep sleep state, and the third term is the energy cost during the deep sleep. Finally the last line represents the additional energy cost included in the above lines which needs to be adjusted. The deep sleep and light sleep detailed calculations are given in the section A.1 of Appendix for reference. In (3.11), we identify the summation part to be an arithmetic-geometric progression and the

simplified expression is given by

$$
\begin{aligned}
E^{\text{edrx}}_{\text{No-WUS}} =& P_{\text{drup}}T_{\text{drup}} + P_{\text{M}}T_{\text{ds-drift}} + P_{\text{M}}T_{\text{sync}}R_{\text{sync}} \\
&+ (1-p_{\text{p}})n(P_{\text{lrup}}T_{\text{lrup}} + P_{\text{M}}T_{\text{ls-drift}} + P_{\text{M}}T_{\text{m}}R_{\text{m}} + P_{\text{lrdwn}}T_{\text{lrdwn}}) \\
&+ p_{\text{tp}}\Bigg[\left(\frac{n\alpha^{n+1} - (n+1)\alpha^{n} + 1}{(1-\alpha^{n})(1-\alpha)}\right)(P_{\text{lrup}}T_{\text{lrup}} + P_{\text{M}}T_{\text{ls-drift}} + P_{\text{M}}T_{\text{m}}R_{\text{m}} \\
&+ P_{\text{lrdwn}}T_{\text{lrdwn}}) + P_{\text{M}}(T_{\text{prt}} + T_{\text{p}}R_{\text{p}})\Bigg] \\
&+ p_{\text{ntp}}\Bigg[n(P_{\text{lrup}}T_{\text{lrup}} + P_{\text{M}}T_{\text{ls-drift}} + P_{\text{M}}T_{\text{m}}R_{\text{m}} + P_{\text{lrdwn}}T_{\text{lrdwn}}) \\
&+ p_{\text{d}} \cdot P_{\text{M}}(T_{\text{prt}} + T_{\text{p}}R_{\text{p}})\Bigg] \\
&+ (1-p_{\text{p}})p_{\text{fa}}\big[nP_{\text{M}}(T_{\text{prt}} + T_{\text{p}}R_{\text{p}})\big] \\
&+ P_{\text{ls}}T^{\text{edrx}}_{\text{ls}} + P_{\text{drdwn}}T_{\text{drdwn}} + P_{\text{ds}}T^{\text{edrx}}_{\text{ds}} \\
&- P_{\text{M}}(T_{\text{ls-drift}} + P_{\text{lrup}}T_{\text{lrup}} + P_{\text{lrdwn}}T_{\text{lrdwn}}).
\end{aligned}
\tag{3.12}
$$

The average power consumed in one eDRX cycle for No-WUS case is calculated with (3.1) using the calculated energy consumed and the corresponding time period of operation.

3.3.2 MWUS: Power Consumption

For the MWUS case in eDRX cycle, similar to DRX cycle, we follow the state diagram as shown in Figure 3.5. In this state diagram, the difference with the No-WUS case is inclusion of the WUS operational state. In this case, once the UE acquires synchronization with the eNodeB using the new RSS signal, it first listens for the WUS. On detecting a correct WUS, the UE continues to read MPDCCH. With inclusion of the WUS, only the intended group of UEs continue to read MPDCCH while the rest of the UEs continue to sleep and thus the energy consumption of the UEs to read MPDCCH unnecessarily is reduced to some extent. This overhearing can only be restricted for non-target groups of UEs. The UEs within the same target group wake up and the overhearing energy cost for them cannot be avoided. If a WUS is not detected, the UE goes to sleep state. Similar to the previous cases, noise or WUSs for other UE groups can be detected as WUS i.e., false alarm may occur and the UE idle listens to the channel and this cost is unavoidable.

On detecting a WUS, the UE can find the paging message in any of the DRX cycles as discussed in the No-WUS case. The same probabilities are considered here to calculate the energy cost based on the outcome of WUS operational state. The average power consumption for MWUS case is calculated using (3.1). The average UE energy consumed in eDRX mode for the MWUS case is calculated

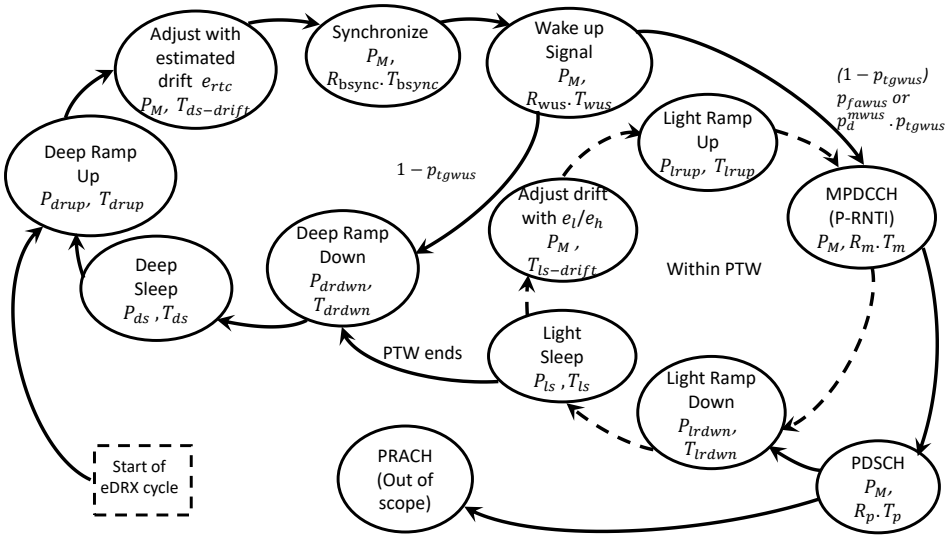

Figure 3.5: State diagram for eDRX cycling with WUS received by MRx

using the expression given by

$$
\begin{aligned}
E_{\text{MWUS}}^{\text{edrx}} =& P_{\text{drup}}T_{\text{drup}} + P_{\text{M}}T_{\text{ds-drift}} + P_{\text{M}}T_{\text{bsync}}R_{\text{bsync}} + P_{\text{M}}T_{\text{wus}}R_{\text{wus}} \\
&+ p_{\text{d}}^{\text{mwus}} \cdot p_{\text{tgwus}} \Bigg[\left(\frac{n\alpha^{n+1} - (n+1)\alpha^n + 1}{(1-\alpha^n)(1-\alpha)} \right) (P_{\text{lrup}}T_{\text{lrup}} + P_{\text{M}}T_{\text{ls-drift}} \\
&+ P_{\text{M}}T_{\text{m}}R_{\text{m}} + P_{\text{lrdwn}}T_{\text{lrdwn}}) + P_{\text{M}}(T_{\text{prt}} + T_{\text{p}}R_{\text{p}}) \Bigg] \\
&+ (1-p_{\text{tgwus}})p_{\text{fawus}} \Bigg[\text{n}(P_{\text{lrup}}T_{\text{lrup}} + P_{\text{M}}T_{\text{ls-drift}} + P_{\text{M}}T_{\text{m}}R_{\text{m}} \\
&+ P_{\text{lrdwn}}T_{\text{lrdwn}}) \Bigg] \\
&+ P_{\text{ls}}T_{\text{ls}}^{\text{edrx}} + P_{\text{drdwn}}T_{\text{drdwn}} + P_{\text{ds}}T_{\text{ds}}^{\text{edrx}} \\
&- (P_{\text{M}}T_{\text{ls-drift}} + P_{\text{lrup}}T_{\text{lrup}} + P_{\text{lrdwn}}T_{\text{lrdwn}}),
\end{aligned}
\tag{3.13}
$$

where, each line represents the energy contribution of different events. The first line represents the ramp up, drift, sync and reading WUS energy cost. The second and third line consists of the energy consumed in case of a WUS detected governed by a probability $p_{\text{d}}^{\text{mwus}}$ and p_{tgwus} where p_{tgwus} is the probability of occurrence of a target WUS and $p_{\text{d}}^{\text{mwus}}$ is the probability of detecting a WUS by MRx. The fourth and fifth lines represents the energy cost for the error event governed by probabilities $(1-p_{\text{tgwus}})$ and p_{fawus}, where the later is the probability of false alarm of WUS. The fifth line gives the sum of light sleep, ramping down and deep sleep energy costs and finally sixth line gives the additional cost included in the above five lines which needs to adjusted.

Now that we have the power consumption expressions for the reference cases

in eDRX cycle, we continue to find the expressions for delay calculations.

3.3.3 eDRX Delay Calculations

In eDRX cycle, the average delay is comparatively larger than the DRX cycle due to longer sleep times. The expressions are similar to delay calculation in DRX cycle but includes necessary changes in probabilities, sleep time and time to detect paging, with respect to eDRX cycle.

No-WUS case: The delay required for the eNodeB to reach the UE operating in eDRX mode is half the deep sleep time along with the time required for the UE to read the paging message. If the UE misses it in a cycle, then the delay is increased further by a cycle time. Considering this possibility, the average delay for this case is calculated similar to the previous expressions as,

$$\begin{aligned} D^{\text{edrx}}_{\text{No-WUS}} =& \frac{T^{\text{edrx}}_{\text{ds}}}{2} + T_{\text{drup}} + T_{\text{ds-drift}} + T_{\text{sync}}R_{\text{sync}} \\ &+ \left[\left(\frac{n\alpha^{n+1} - (n+1)\alpha^n + 1}{(1-\alpha^n)(1-\alpha)}\right)(T_{\text{lrup}} + T_{\text{ls-drift}} + T_{\text{m}}R_{\text{m}} \right. \\ &\left. + T_{\text{lrdwn}}) + (T_{\text{prt}} + T_{\text{p}}R_{\text{p}})\right] \\ &- (T_{\text{ls-drift}} + T_{\text{lrup}} + T_{\text{lrdwn}}) \\ &+ \frac{(\alpha)(1-\alpha)}{(1-\alpha^n)}\left[(1+2\alpha+3\alpha^2)\left[T^{\text{idrx}} - (T_{\text{lrup}} + T_{\text{ls-drift}} + T_{\text{m}}R_{\text{m}} \right.\right. \\ &\left.\left. + T_{\text{lrdwn}})\right] - (1+\alpha+2\alpha^2)(T_{\text{sync}}R_{\text{sync}} + T_{\text{ds-drift}} - T_{\text{ls-drift}})\right] \\ &+ \left(\frac{1-p_{\text{d}}}{p_{\text{d}}}\right)T^{\text{edrx}}. \end{aligned} \tag{3.14}$$

MWUS case: The delay expression for MWUS case is based on the successful detection of the WUS. If a WUS is missed by a UE, the delay is further increased by a cycle time. The average delay for MWUS case in eDRX operation is calculated

and is given by

$$
\begin{aligned}
D^{\text{edrx}}_{\text{MWUS}} =& \frac{T^{\text{edrx}}_{\text{ds}}}{2} + T_{\text{drup}} + T_{\text{ds-drift}} + T_{\text{bsync}} R_{\text{bsync}} + T_{\text{wus}} R_{\text{wus}} \\
&+ \left[\left(\frac{n\alpha^{n+1} - (n+1)\alpha^n + 1}{(1-\alpha^n)(1-\alpha)} \right) (T_{\text{lrup}} + T_{\text{ls-drift}} + T_{\text{m}} R_{\text{m}} \right. \\
&\left. + T_{\text{lrdwn}}) + (T_{\text{prt}} + T_{\text{p}} R_{\text{p}}) \right] \\
&- (T_{\text{ls-drift}} + T_{\text{lrup}} + T_{\text{lrdwn}}) \\
&+ \frac{(\alpha)(1-\alpha)}{(1-\alpha^n)} \left[(1 + 2\alpha + 3\alpha^2) \left[T^{\text{idrx}} - (T_{\text{lrup}} + T_{\text{ls-drift}} + T_{\text{m}} R_{\text{m}} \right. \right. \\
&\left. \left. + T_{\text{lrdwn}}) \right] - (1 + \alpha + 2\alpha^2)(T_{\text{wus}} R_{\text{wus}} + T_{\text{bsync}} R_{\text{bsync}} + T_{\text{ds-drift}} - T_{\text{ls-drift}}) \right] \\
&+ \left(\frac{1 - p^{\text{mwus}}_{\text{d}}}{p^{\text{mwus}}_{\text{d}}} \right) T^{\text{edrx}}
\end{aligned}
\tag{3.15}
$$

Similar to the calculations for the reference cases, we proceed to derive the equations for energy consumption and delay calculations for our investigated solution.

3.4 WWUS: eDRX Power Consumption

In this section, we discuss the investigated solution, average power consumption and delay calculations. As calculated for UEs operating in DRX cycle, the energy costs for both WRx and MRx are taken into consideration. The total energy cost is given similar to the DRX WWUS case, as an aggregate of the energies consumed by MRx and WRx based on the UE operations.

3.4.1 WWUS: Power Consumption

For the WWUS case during eDRX cycle, we follow the state diagram as shown in Figure 3.6. Here, the WRx duty cycles, listening to the channel for the WUS. On successful detection of a WUS by the WRx, it triggers the MRx to switch on. The UE then performs its operations to further read the MPDCCH and PDSCH accordingly. If a WUS is not detected by the WRx, then it moves back to the sleep state. The energy consumption of the UEs is further reduced in this case, as WRx runs on low power and the MRx is turned on only when the eNodeB needs to communicate with the UE. Further reduction in energy cost can be achieved through new WUS signal design, which is discussed later. Similar to the previous cases, false alarm can resulting in additional unavoidable energy costs. The average energy consumption is calculated by summing up the energy cost components with respect to their probabilities using the power, time, number of repetitions provided in the operational states.

Based on the discussed operation, the average power consumed by the UE for WWUS case is calculated using the (3.1) with the average energy consumed

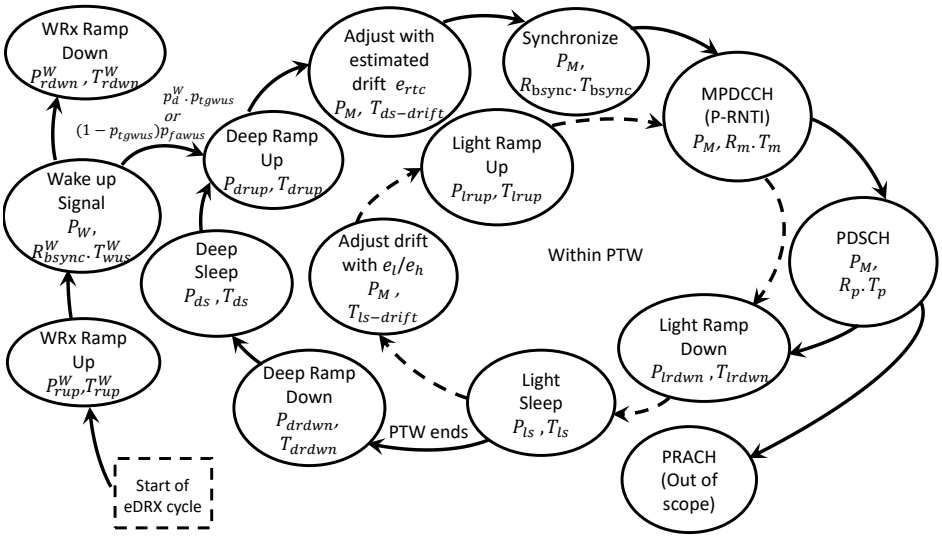

Figure 3.6: State diagram for eDRX cycling with WUS received by WRx

calculated using the expression,

$$\begin{aligned}
E^{\text{edrx}}_{\text{WWUS}} =& E^{\text{W}}_{\text{wus}} + p_{\text{tgwus}} \cdot p^{\text{W}}_{\text{d}} \Big[P_{\text{drup}} T_{\text{drup}} + P_{\text{M}}(T_{\text{ds-drift}} + T_{\text{bsync}} R_{\text{bsync}}) \\
&+ \Big[\Big(\frac{n\alpha^{n+1} - (n+1)\alpha^n + 1}{(1-\alpha^n)(1-\alpha)} \Big) (P_{\text{lrup}} T_{\text{lrup}} + P_{\text{M}} T_{\text{ls-drift}} + P_{\text{M}} T_{\text{m}} R_{\text{m}} \\
&+ P_{\text{lrdwn}} T_{\text{lrdwn}}) + P_{\text{M}}(T_{\text{prt}} + T_{\text{p}} R_{\text{p}}) \Big] \\
&- (P_{\text{M}} T_{\text{ls-drift}} + P_{\text{lrup}} T_{\text{lrup}} + P_{\text{lrdwn}} T_{\text{lrdwn}}) + P_{\text{drdwn}} T_{\text{drdwn}} \Big] \\
&+ (1 - p_{\text{tgwus}}) p^{\text{W}}_{\text{fawus}} \Big[P_{\text{drup}} T_{\text{drup}} + P_{\text{M}}(T_{\text{ds-drift}} + T_{\text{bsync}} R_{\text{bsync}}) \\
&+ \text{n}(P_{\text{lrup}} T_{\text{lrup}} + P_{\text{M}} T_{\text{ls-drift}} + P_{\text{M}} T_{\text{m}} R_{\text{m}} + P_{\text{lrdwn}} T_{\text{lrdwn}}) \\
&- (P_{\text{M}} T_{\text{ls-drift}} + P_{\text{lrup}} T_{\text{lrup}} + P_{\text{lrdwn}} T_{\text{lrdwn}}) + P_{\text{drdwn}} T_{\text{drdwn}} \Big] \\
&+ P_{\text{ls}} T^{\text{edrx}}_{\text{ls}} + P_{\text{ds}} T^{\text{edrx}}_{\text{ds}},
\end{aligned} \tag{3.16}$$

where, each line represents different cost elements which sum up to give the total average energy cost, similar to the previous cases. WRx correctly detects the WUS with the probability p^{W}_{d} and the false alarm probability of WRx is given by $p^{\text{W}}_{\text{fawus}}$.

3.4.2 WWUS: Delay Calculation

In this subsection, we express the delay calculation for WWUS case, similar to reference cases but the difference compared to reference cases, is the detection

probability applicable here, $p_{\mathrm{d}}^{\mathrm{W}}$ for WRx. The delay for WWUS case is given by

$$\begin{aligned} D_{\mathrm{avg}}^{\mathrm{edrx}} =& \frac{T_{\mathrm{ds}}^{\mathrm{edrx}}}{2} + T_{\mathrm{rup}}^{\mathrm{W}} + T_{\mathrm{drift}}^{\mathrm{W}} + R_{\mathrm{wus}}^{\mathrm{W}} T_{\mathrm{wus}}^{\mathrm{W}} + T_{\mathrm{rdwn}}^{\mathrm{W}} + T_{\mathrm{switch}} + T_{\mathrm{drup}} + T_{\text{ds-drift}} \\ & + T_{\mathrm{bsync}} R_{\mathrm{bsync}} + \left[\left(\frac{n\alpha^{n+1} - (n+1)\alpha^n + 1}{(1-\alpha^n)(1-\alpha)} \right) (T_{\mathrm{lrup}} + T_{\text{ls-drift}} + T_{\mathrm{m}} R_{\mathrm{m}} \right. \\ & \left. + T_{\mathrm{lrdwn}}) + (T_{\mathrm{prt}} + T_{\mathrm{p}} R_{\mathrm{p}}) \right] \\ & - (T_{\text{ls-drift}} + T_{\mathrm{lrup}} + T_{\mathrm{lrdwn}}) \\ & + \frac{(\alpha)(1-\alpha)}{(1-\alpha^n)} \left[(1 + 2\alpha + 3\alpha^2) \left[T^{\mathrm{idrx}} - (T_{\mathrm{lrup}} + T_{\text{ls-drift}} + T_{\mathrm{m}} R_{\mathrm{m}} \right. \right. \\ & \left. \left. + T_{\mathrm{lrdwn}}) \right] - (1 + \alpha + 2\alpha^2)(T_{\mathrm{bsync}} R_{\mathrm{bsync}} + T_{\text{ds-drift}} - T_{\text{ls-drift}}) \right] \\ & + \left(\frac{1 - p_{\mathrm{d}}^{\mathrm{W}}}{p_{\mathrm{d}}^{\mathrm{W}}} \right) T^{\mathrm{edrx}}. \end{aligned} \tag{3.17}$$

During the derivation of the equations for the energy consumption and delay, we consider an important parameter, UE clock drift with respect to the eNodeB clock. Let us now look at the estimation of this drift calculation.

3.5 Estimated drift time calculation

To avoid missing the signals from eNodeB, enough margin against clock drift needs to be added as time drift and the UE should turn on earlier than what its clock indicates. This time margin is estimated based on the sleep time of the UE. The drift calculation when the UE ramps up from sleep is given by,

$$T_{\text{ls-drift}} = 0.5 e_x (T_{\mathrm{sleep}})^{\mathrm{y}} \quad \mu\mathrm{s}, \tag{3.18}$$

where e_x is the estimated correction factor which depends on the UE sleep time T_{sleep} and the y varies with respect to the correction factor [1].

When the UE ramps up from light sleep, the correction factor takes two values given by e_{l} and e_{h}, representing the low and high correction factors. The degree y of the sleep time takes the value one, if the correction factor is e_{h} and two, if the correction factor is e_{l}. When the UE ramps up from deep sleep, the drift time is estimated with the correction factor e_{rtc} and the MRx deep sleep duration in the previous cycle. Similar to MRx, the WRx also has to wake up earlier in order to adjust its clock with the eNodeB clock. This drift time is estimated using the error correction factor for WRx $e_{\mathrm{rtc}}^{\mathrm{W}}$ and the previous cycle sleep duration of the WRx.

Along with the derived equations for power consumption and delay calculations, these drift calculations are also required to evaluate the relative power saving with our investigated solution and this is discussed in Chapter 5. Apart from the equations, designing a WUS for the WRx and the probabilities of detection, false alarm of WRx need to be evaluated. We now proceed to design a suitable WUS, perform simulations to find out the detection and false alarm probabilities of WRx in the next chapter.

Chapter 4

Design considerations for the WUS

In this chapter, we design a new WUS, suitable for the WRx. As discussed earlier, the introduction of WRx comes with a performance loss. To reduce the effect of such loss, we design new WUS so that it can withstand high bit-error rates which comes in as a result of the performance loss of the WRx. In the energy consumption expressions, the values of detection and false alarm probabilities along with the sequence lengths, play an important role, as they strongly influence the UE's total energy consumption. We analyze each WUS design, simulate its performance and finally, tabulate the values of probabilities of detection and false alarm using the Receiver Operational Characteristics (ROC) curves of WRx with respect to the considered bit error rates. In general, a typical receiver design includes an Analog Front End (AFE) and Digital Base Band (DBB) processing unit. The AFE receives the transmitted signals from eNodeB and converts it into digital bit streams, which are fed to the DBB for further analysis. Our focus in this chapter is to design a WUS and propose the corresponding DBB required. Another important aspect to be considered, while designing the WUS, is the time required for the UE to remain ON to receive a WUS and detect it. This is relate-able with the length of WUS design and also the repetitions required to detect it properly, for a UE located far away from the eNodeB. With distance, the probability of bit error of the received signal increases. In this chapter, we examine the performance of the designed WUS in extended coverage area by investigating the number of repetitions required to detect the WUS at high bit error rates.

Hence, when the UE is operating far away from the eNodeB, it is difficult to receive the WUS and we need more repetitions, which ends up in increasing the ON time of the WRx which is undesirable.

4.1 Structure

In this section, we analyze the different WUS design structures which are considered and the advantages of each design over others. First we discuss the information to be sent through this signal. As discussed earlier, the UEs camp on to an eNodeB and irrespective of UE being stationary or mobile it is beneficial if the UE can identify the current eNodeB it wants to talk. Hence, the idea of including the Physical Cell Identity (PCI) information, which provides unique identity of the eNodeBs, as part of our WUS design is advantageous. As shown in Figure 4.1(a),

our first design consists of PCI information. To avoid the waking up of UEs by detecting the WUS sent by the neighbouring eNodeBs, PCI information is necessary to be present in the WUS. Here, when a WUS is sent by the eNodeB, all the UEs listening to the eNodeB at that instant wakes up. This design is only beneficial if the requirement is to wake up all the UEs camped on to a particular eNodeB. In case the requirement is to wake up certain group of UEs out of all the UEs listening to the WUS in the same cell, we can achieve it by forming Wake-up Groups (WUG)s. WUGs allows us to wake up only the UEs belonging to a certain group camped on to the same eNodeB. Group identity information can be included in the WUS as second segment of information along with PCI. This forms the basis of our second design structure and is shown in Figure 4.1(b). This design is an effective solution for reducing energy cost due to overhearing. Now, if we divide the PCI information into two parts, i.e., cell group ID and cell ID, and represent them with individual sequences, which we discuss later, we can increase the number of possible WUGs. This strategy is implied for our third design structure as shown in Figure 4.1(c). If WUS is designed to address individual UEs by including Unique Wake-up Identity (WUID), it eradicates the loss due to overhearing. But this approach makes the WUS signal length quite long which leads to long processing time. Focusing on these three design structures, let us understand the design principle of WUS in the next section.

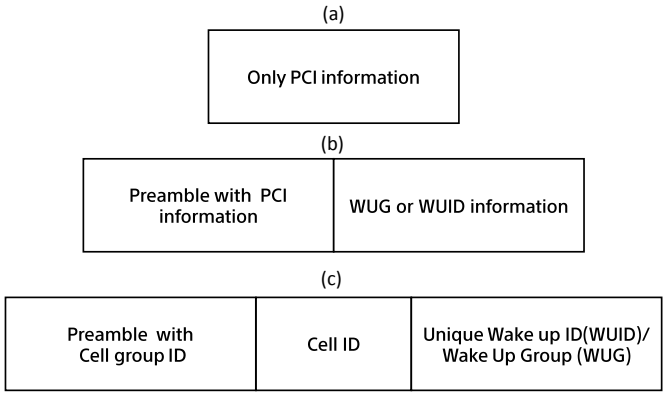

Figure 4.1: WUS design structures

4.2 Principle

In general, the basic principle behind the WUS design is to design a signal which can be easily detected by non-coherent receivers. As discussed in earlier chapters, we select the binary pseudo-random sequences as the basis of WUS design. It is advantageous to have the cell identification and wake up identity sections of the WUS be represented by the chosen sequences. For the matched filter of the DBB processing unit, it is easy for the DBB processing unit to detect a sequence of bits representing single bit information compared to decoding bit by bit transmitted

information bits. The detection capability of WRx is not comparable with the MRx on the whole, which is a radio frame synchronized coherent receiver. The pseudo-random sequences are chosen from the sequences with good auto and cross correlation properties which reduces the probability of false alarm and increases the probability of detection of WUS by WRx. It makes the ROC of WRx comparable to the ROC of MRx. The WRx, being non-coherent is likely to detect such sequences with greater precision along with saving the energy to sync. We focus to keep the WUS length as short as possible as we intend to use this solution also for those UEs in the bad coverage conditions. When the UE is far away from the eNodeB, it requires several repetitions to read the signal. So the effect of low power consumption of the WRx will get scaled down due to longer ON time to receive WUS.

To understand the ROC curve, Figure 4.2 is shown with different areas specified. The points on the ROC curve in areas 1 and 2 have better p_{d} compared to that of areas 3 and 4. We intend to choose the points in area 1 as they have higher p_{d} and lower p_{fa}. Now, that we have understood the design principle, lets discuss in detail about each WUS design in the following sections.

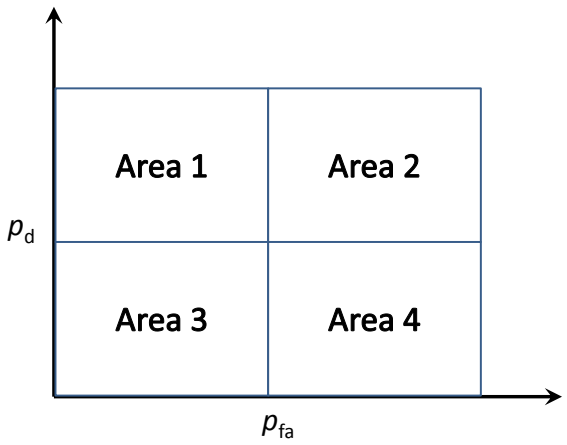

Figure 4.2: Regional description of the ROC curve

4.3 Including PCI information

The first design of WUS consists of only PCI information transmitted from respective eNodeB as shown in Figure 4.1(a). In the cellular network, the coverage areas are broadly divided into cells according to their physical locations. A cell is identified with its respective eNodeB. There are 504 possible cell identities and for simplicity they are divided into 168 cell groups, each with three cell IDs (0, 1 and 2). This information is unique for each eNodeB within that coverage area. To

transmit PCI information through WUS, we need 504 different sequences to represent each PCI. With the help of this WUS design, the UE camped on or located in a particular cell, can identify communication with its respective eNodeB and avoid reading signals from neighbouring eNodeBs. For this type of WUS design, it is also important to know the DBB which needs to be present to process the input bit stream from AFE. Let us focus on the DBB, in the next subsection.

4.3.1 Digital baseband

In a DBB, the Cell-identity Matched Filter (CMF), is a correlator, and it detects the PCI based on the sequence pattern which is known to the receiver. A correlator has a previously stored sequence of bit stream of certain finite length and it matches the pattern with incoming bit stream from AFE. If a peak above the preconceived threshold occurs, it considers the event to be a correct detection. The DBB for the WUS design with only PCI information consists of only one segment as shown in Figure 4.3. It is basically a matched filter or correlator which matches the received bit sequence with the bit pattern representing the eNodeB to which the UE has camped on.

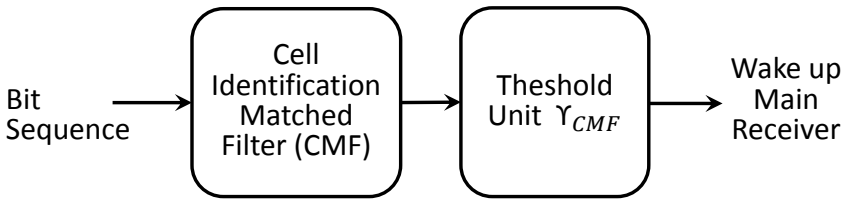

Figure 4.3: DBB design with sequences used in WUS with PCI

For this type of detection technique, we have to be careful about the signal design so that the WRx does not detect a wrong signal to be the correct one. Hence, for such design, the prime factor is sequence selection, which is covered in the following subsection.

4.3.2 Sequence Selection

In this subsection, we look at different combinations of the binary pseudo-random sequences in the above discussed WUS design structures and select specific se-

quences based on their auto and cross correlation properties.

We investigated multiple sequences namely, Zadoff-Chu, Gold, Kasami, Barker and maximum length sequences, and they show good auto and cross correlation properties. Among these sequences, we choose the ones which shows good correlation properties and has minimum length. As discussed in earlier chapters, the sequences with such properties improves the probability of detection of WRx and lowers the false alarm rate. Among the above mentioned sequences, we select Kasami sequence of length sixty-three (63), since it shows very good correlation properties as shown in Figure 4.4 and also it is possible to generate 520 different Kasami sequences of length sixty-three. Hence, it can represent 504 different PCIs easily. Moreover, it is the minimum length possible to represent the PCI information with the sequences we have investigated.

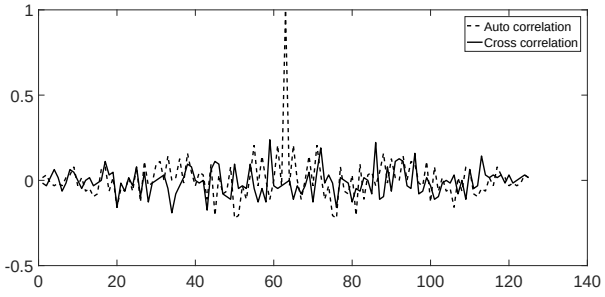

Figure 4.4: Auto and Cross-correlation of Kasami Sequence of length 63

In order to evaluate the performance of selected sequences, we need to further verify by simulating the WUS design using Monte Carlo algorithm and the results are discussed in the below subsection.

4.3.3 Simulation of the WUS design

We plot the ROC curves for the different probabilities of bit error and analyze the performance of the receiver. According to the ROC curves, an increase in bit error probability p_{b} from 0.05 to 0.15 leads to a decrease in p_{d} and increase in p_{fa}.

If we focus on the figure 4.5(b), which is the ROC curve showing detection probability versus false alarm probability at different thresholds, we notice that the performance remains quite good and the probability of detection is almost 100% above a threshold of 40% of the length of sequence, i.e., 28. The false alarm is very high in the region where the threshold, γ_{CMF} is less than 28. Any threshold, between 28 to 40, is ideal for the bit error probabilities 0.05 and 0.1. But for bit error probability 0.15, the range of γ_{CMF} is between 28 and 32, as we can see that the performance degrades at higher thresholds. So one has to be cautious in selecting the threshold with respect to the p_{b}. Similarly, Figure 4.5(a) shows the ROC plot with p_{d} versus the probability of false alarm due to detection of other cell WUS. We see at the threshold of 28, p_{d} of 0.9862 and p_{fa} of 0.0532 for a bit

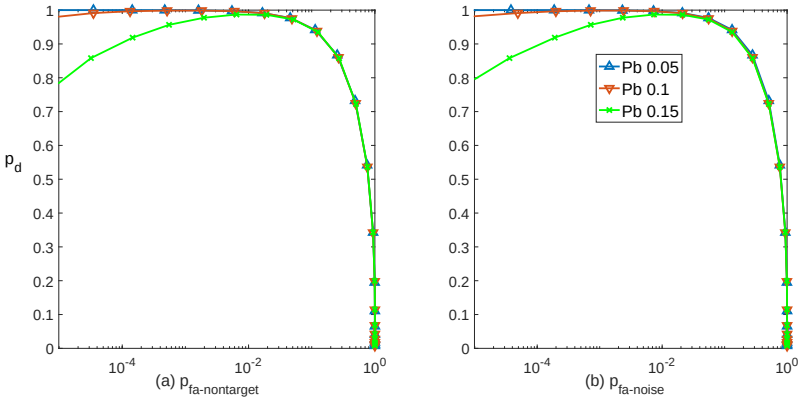

Figure 4.5: ROC plot for WUS with PCI representing p_{d} vs probability of non-target false alarm, $p_{\text{fa-nontarget}}$ and probability of noise false alarm $p_{\text{fa-noise}}$

Table 4.1: Simulation results - WUS with PCI

p_{b}	p_{d}	p_{fa}
0.05	0.9972	0.0072
0.1	0.9968	0.0074
0.15	0.9869	0.0074

error probability of 0.05. This means probability of signal detection of WRx is 98.62% whereas the false alarm rate is 5.3%.

Considering the threshold to be 30, for further calculations, the corresponding p_{d} and p_{fa} values with respect to the selected p_{b}s are tabulated in Table 4.1.

4.4 Including PCI and WUG information

In the previous design, we notice that the UEs wake up even when the WUS is intended to wake up other devices. To address this issue, we have a different approach in this WUS design. This design facilitates grouped wake up of UEs, to reduce unnecessary overhearing energy loss. The WUS design consists of two segments, PCI information in one and UE group identity information on the other as shown in Figure 4.1(b) and each segment is represented by a sequence. The principle behind this design is that the UEs within a single PCI, wake up with respect to their WUGs. Although this approach does not eradicate the overhearing energy cost totally, it limits this energy cost to a certain level. The UE first checks the PCI and then authenticates the WUG before triggering MRx to switch on. The DBB processing unit for this WUS design can be of different types depending on the number of preferred WUGs which we discuss in the following subsection.

4.4.1 Digital baseband

The DBB consists of two segments as shown in Figure 4.6. The first segment is similar to DBB of the previous WUS design and the next segment is a correlator to recognize the UE identity called as Identity De-Spreader (IDS). The IDS decodes the WUG information and confirms if the WRx should trigger the MRx.

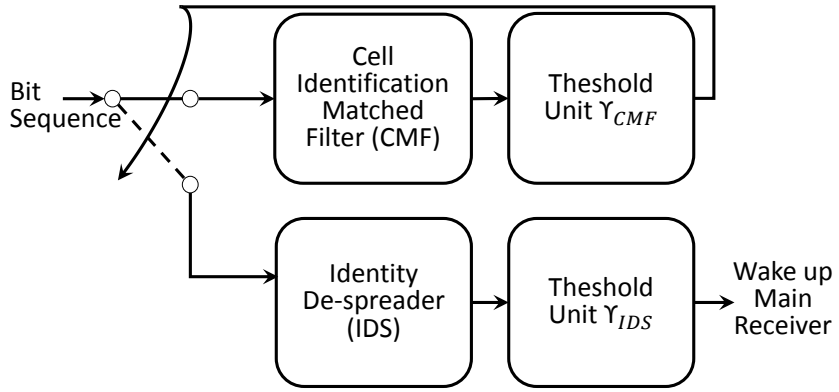

Figure 4.6: DBB design for WUS with PCI and WUG

Now that we are aware of the type of DBB we propose, and each segment being an individual sequence, we continue to discuss the sequence selection for these two segments in the next sub section.

4.4.2 Sequence Selection

The sequence selection for this design follow the same principle as discussed in the first design. Sixty-three length Kasami sequence is used for PCI information in the first section and for the next section, we analyze the performance of other sequences or Kasami itself and its limitation to number of WUGs. The first consideration is Kasami sequence for IDS part and the limitation with such use is that 504 out of 520 sequences are dedicated for PCI. Hence, remaining sixteen sequences can represent sixteen WUGs.

The other option for IDS part is to use thirty-one length Gold sequence which shows similar correlation properties and it also reduces the WUS length to ninety-four, compared to the case with two sixty-three length Kasami sequences. With this kind of design, thirty-one WUGs can be addressed which is almost twice the WUGs addressed compared to using two Kasami sequences.

With the same design structure, another combination is considered i.e. a preamble segment of sixty-three length Kasami with two consecutive m-sequences for addressing four WUGs. Two different m-sequences of length fifteen with good correlation properties can be generated. One represents binary '0' in WUG address and another represents '1'. This WUS design is of the shortest length, ninety-three.

Table 4.2: Bit representation of WUG address information

WUG ID	WUG address
00	1
01	2
10	3
11	4

Table 4.3: Simulation results - WUS with PCI and WUG design 1

p_{b}	p_{d}	p_{fa}
0.05	0.9935	10^{-5}
0.1	0.9931	$9 \cdot 10^{-6}$
0.15	0.9731	$6 \cdot 10^{-6}$

With all these three possible designs for this WUS structure, we now simulate to find the p_{d} and p_{fa} values by plotting the ROC curves of the respective designs.

4.4.3 Simulation of the WUS designs

First, we simulate the case of two Kasami sequences and analyze the result. The ROC curves shown in Figure 4.8, gives a promising result for the range of γ_{CMF} from 28 to 32. For the IDS part, we consider a pdf plot shown in Figure 4.7, which shows with γ_{IDS} as 30, the address part is detected with highest p_{d} and lowest p_{fa}.

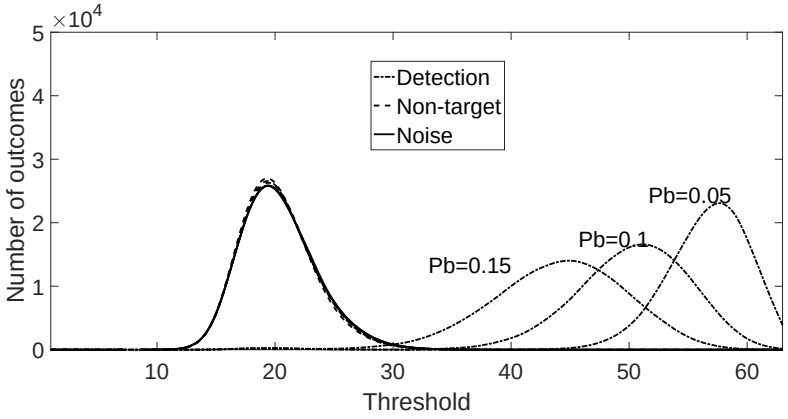

Figure 4.7: PDF plot to select threshold for Kasami sequence of length 63

Considering the γ_{CMF} and γ_{IDS} for operating our WRx to be 30, the corresponding p_{d} and p_{fa} values for the respective p_{b} are shown in the Table 4.3.

For the second case, we have a preamble Kasami sequence and identity Gold

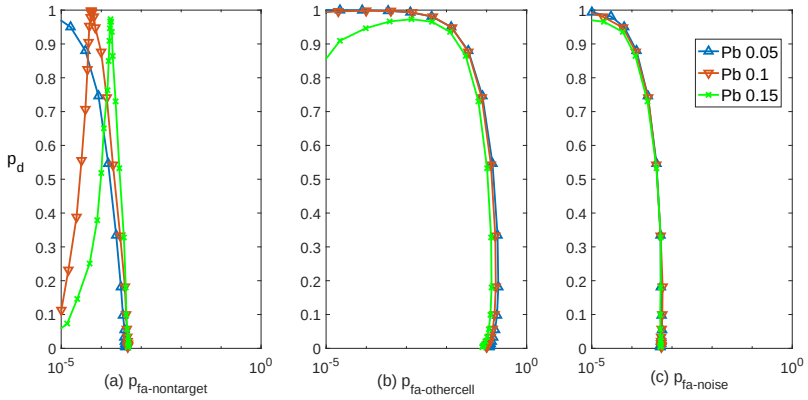

Figure 4.8: ROC plot for WUS with PCI and WUG - Design 1 representing p_{d} vs probability of non-target false alarm $p_{\text{fa-nontarget}}$, probability of other-cell false alarm $p_{\text{fa-othercell}}$ and probability of false alarm due to noise $p_{\text{fa-noise}}$

sequence. The simulation results are similar to the previous case, two segments of Kasami sequences, with desired results when γ_{CMF} ranges from 28 to 32. For the IDS section, from the pdf plot shown in Figure 4.9, we observe that if the γ_{IDS} is considered as 15, we have maximum p_{d} and minimum p_{fa}. The results are shown in Figure 4.10.

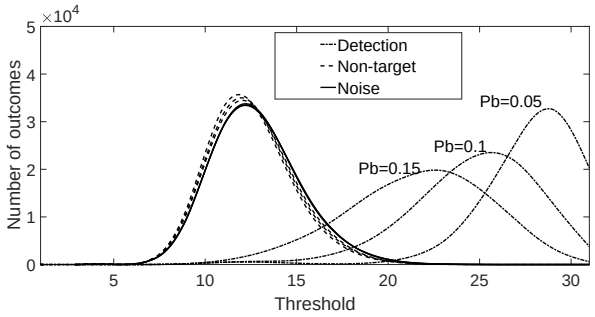

Figure 4.9: PDF plot to select threshold for Gold Sequence of length 31

Considering the γ_{CMF} to be the same, 30 and γ_{IDS} to be 15, the corresponding p_{d} and p_{fa} values for the respective p_{b} are shown in the Table 4.3.

For the third case, Kasami sequence of length sixty-three is used as the preamble and two m-sequences are used for the address identification. The threshold for m-sequences is chosen to be 8 for the sections IDS-1 and IDS-2, based on the pdf plot as shown in Figure 4.11. The simulation results for this design are shown in Figure 4.12.

With the chosen γ_{IDS} for both sections as 8 and the γ_{CMF} as 30, the corre-

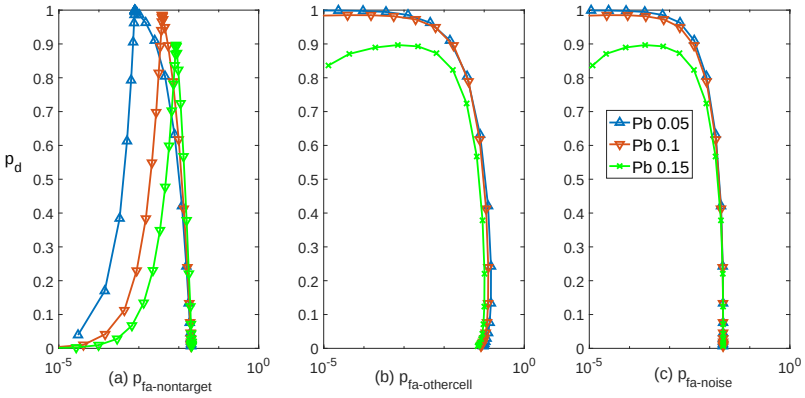

Figure 4.10: ROC plot for WUS with PCI and WUG - Design 2 representing p_{d} vs probability of non-target false alarm $p_{\text{fa-nontarget}}$, probability of other-cell false alarm $p_{\text{fa-othercell}}$ and probability of false alarm due to noise $p_{\text{fa-noise}}$

Table 4.4: Simulation results - WUS with PCI and WUG design 2

p_{b}	p_{d}	p_{fa}
0.05	0.9945	0.00024
0.1	0.9819	0.00025
0.15	0.8968	0.00025

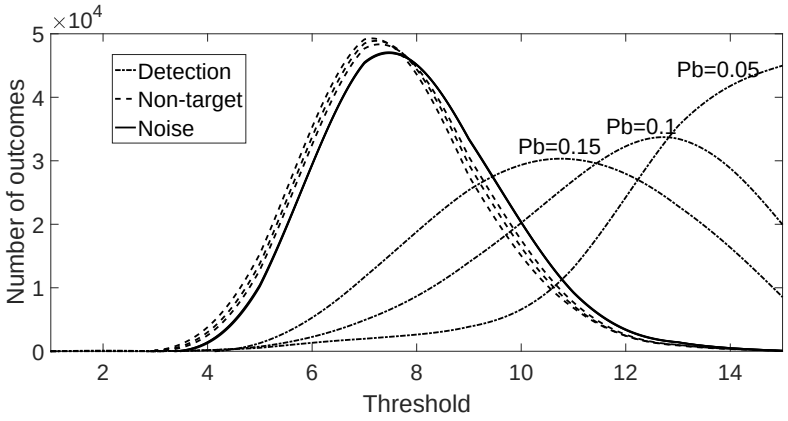

Figure 4.11: PDF plot to select threshold for m-Sequence length 15

sponding p_{d} and p_{fa} values for the respective p_{b} are shown in the Table 4.5.

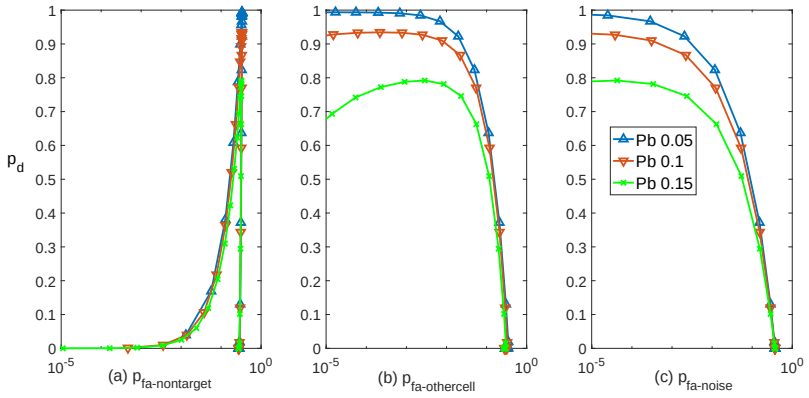

Figure 4.12: ROC plot for WUS with PCI and WUG - Design 3 representing p_{d} vs probability of non-target false alarm $p_{\text{fa-nontarget}}$, probability of other-cell false alarm $p_{\text{fa-othercell}}$ and probability of false alarm due to noise $p_{\text{fa-noise}}$

Table 4.5: Simulation results - WUS with PCI and WUG design 3

p_{b}	p_{d}	p_{fa}
0.05	0.9844	$2.5 \cdot 10^{-5}$
0.1	0.9271	$3.8 \cdot 10^{-5}$
0.15	0.7919	$4.3 \cdot 10^{-5}$

4.5 Including splitted PCI and WUG information

The third structure for WUS consists of 3 parts, preamble representing 168 cell group IDs, second part representing 3 cell IDs and third part representing the WUG or WUIDs as shown in Figure 4.1(c). This type of design is suitable when we need a larger number of WUGs. This design reduces the energy cost due to overhearing further. The DBB components are discussed in detail in the next subsection.

4.5.1 Digital baseband

The DBB for this design is shown in Figure 4.13. This design is suitable for addressing the highest number of WUGs discussed so far. It can address UEs individually as well, depending on the sequence selection and number of sequences representing UE address identity.

4.5.2 Sequence Selection

According to our investigation, the design compatible to this structure is three 63 length Kasami sequences, each for the three individual segments. Sending three sequences of length 63, can address 349 WUGs or 349 WUIDs. Out of 520

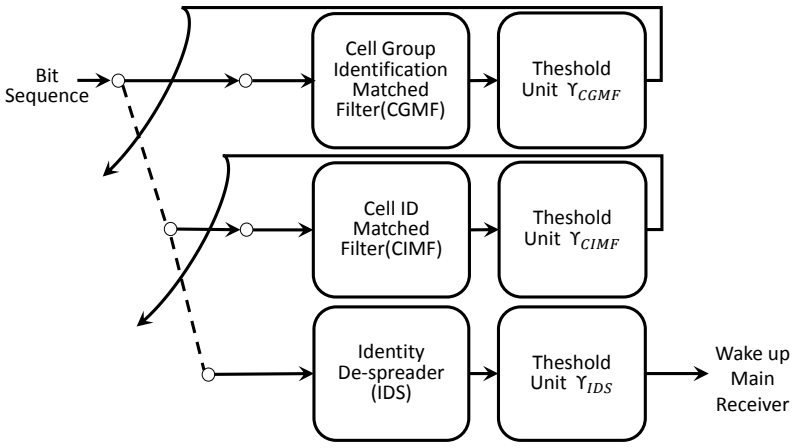

Figure 4.13: DBB design for WUS with PCI and WUID

sequences, 168 are used for cell group ID in the first segment and 3 sequences are used for cell ID in the second segment.

Now that we have understood the design that we are proposing here, let us analyze the simulation result of the same in the next subsection.

4.5.3 Simulation of WUS design

For simulating this case, we consider γ_{IDS} to be 30 for the Kasami sequences as we have considered for the previous cases. The ROC curves generated with the simulation of the WUS design are shown in Figure 4.14.

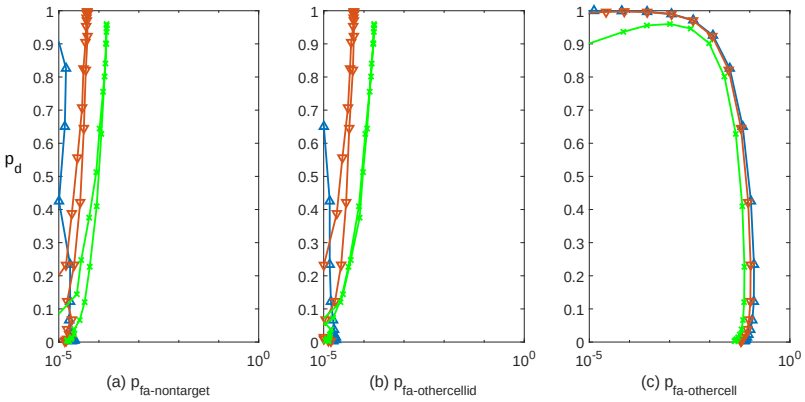

Figure 4.14: ROC plot for WUS with splitted PCI and WUG representing p_{d} vs probability of non-target false alarm $p_{\text{fa-nontarget}}$, probability of other-cell ID false alarm $p_{\text{fa-othercellid}}$ and probability of other cell false alarm $p_{\text{fa-othercell}}$

Table 4.6: Simulation results - WUS with splitted PCI and WUG

p_{b}	p_{d}	p_{fa}
0.05	0.9901	$7 \cdot 10^{-6}$
0.1	0.9895	$5.1 \cdot 10^{-5}$
0.15	0.9599	$1.5 \cdot 10^{-4}$

From the results, we can observe that results are better for γ_{CMF} ranging from 28 to 32. Considering the γ_{CMF} and γ_{IDS} for operating our WRx to be 30, the corresponding p_{d} and p_{fa} values for the respective p_{b} are shown in the Table 4.6.

4.6 Proposed WUS design

Here, we tabulate the different type of WUS designs with respect to the p_{d}, p_{fa}, length of the sequence (L), number of groups (G) and processing time(T) in the following Table 4.7. The segregation is mainly based on the WUS design structure.

Table 4.7: Consolidated simulation results

WUS Design	L	G	p_{b}	p_{d}	$p_{\mathrm{fanoise}}/p_{\mathrm{faNT}}/p_{\mathrm{faOC}}/p_{\mathrm{faOCID}}$	T(ms)
PCI only	63	1	0.05	0.9972	0.0072/0.0054/n.a/n.a	0.2857
			0.1	0.9968	0.0074/0.0059/n.a/n.a	
			0.15	0.9869	0.0074/0.0064/n.a/n.a	
PCI and Group Address	126	16	0.05	0.9935	$10^{-5}/9 \cdot 10^{-5}/0.0013$/n.a	0.5714
			0.1	0.9931	$9 \cdot 10^{-6}/5.9 \cdot 10^{-6}/0.0014$/n.a	
			0.15	0.9731	$6 \cdot 10^{-6}/0.17 \cdot 10^{-3}/0.0013$/n.a	
	94	31	0.05	0.9945	$0.00024/0.00087/3.5 \cdot 10^{-4}$/n.a	0.4286
			0.1	0.9819	$0.00025/0.0039/5.5 \cdot 10^{-4}$/n.a	
			0.15	0.8968	$0.00025/0.0086/7.01 \cdot 10^{-4}$/n.a	
	93	4	0.05	0.9844	$2.5 \cdot 10^{-5}/0.3331/0.0022$/n.a	0.4286
			0.1	0.9271	$3.8 \cdot 10^{-5}/0.3313/0.0025$/n.a	
			0.15	0.7917	$5.3 \cdot 10^{-5}/0.32/0.0029$/n.a	
Splitted PCI and Group Addresses	189	349	0.05	0.9901	$0/7 \cdot 10^{-6}/0.0011/5 \cdot 10^{-6}$	1
			0.1	0.9895	$0/5.1 \cdot 10^{-5}/0.0011/5.6 \cdot 10^{-5}$	
			0.15	0.9599	$0/1.5 \cdot 10^{-4}/0.0010/1.7 \cdot 10^{-4}$	

The table enlists the characteristics of the different WUS designs. The first design is not acceptable due to the overhearing energy cost, so to choose between the second and third designs, the WUS design with PCI and group address is reasonable as the length of WUS is lower than that of the WUS design with splitted PCI and WUG. We have three options in that selection, out of which the WUS design with two Kasami sequences has the maximum detection probability compared to the other designs and low false alarm probabilities. We proceed with our analysis considering the WUS design with two Kasami sequences as our preferred design.

The WUS design is capable of handling 16 WUGs and with error probability 0.15, the percentage of detection is 97.3% with false alarm quite low. The bit error probability for receiving WUS by WRx is more than MRx as discussed earlier. In cellular networks, the total loss in signal strength from eNodeB to the UE is termed Maximum Coupling Loss (MCL). Earlier while deriving the energy consumption equations, we considered the repetitions for detecting a signal. This is to achieve

Table 4.8: Consolidated simulation results of selected design with higher probability of bit error

	p_{b}=0.15	p_{b}=0.20	p_{b}=0.25	p_{b}=0.30	p_{b}=0.35
R	1	2	3	5	10
p_{d}	97.9	99.8	99.6	99.1	99.6
γ_{CMF}	30	48	60	86	124
γ_{IDS}	28	40	54	74	109
p_{fa}	0.002	0.007	0.0075	0.0053	0.006

the required SNR through repetitions. The SNR varies with the distance of the UE from the eNodeB and the distance of UE from eNodeB is expressed in terms of MCL. In LTE, the 3GPP standard representation of MCL, ranges from 144 dB to 164 dB, where 144 dB is the loss in signal strength for the normal coverage condition and 164 dB is the loss in signal strength for extended coverage conditions. The bit error probability of 0.15 corresponds to an MCL of 144 dB. Following (4.1), we find that the corresponding bit error rate for MCL 149 dB is 0.35. In case, power boosting of 6 dB is applied to the transmitted signal, the operating range of the solution get increased from 149 dB MCL to 155 dB MCL. However, in our analysis we consider the operating range upto 149 dB MCL only.

$$p_{\mathrm{b}} = 0.5 \cdot e^{-SNR \cdot \mathrm{k}} \tag{4.1}$$

In (4.1), k is the constant dependent on WRx design. Hence, we analyze the design further with higher error probabilities and simulate its performance. The design continues to show good performance at higher error probabilities with added repetitions. The chosen solution works well until a probability of bit error of about 0.35, beyond this point, the number of required repetitions increase rapidly and makes it impractical. The result corresponding to each bit error probability are given in Table 4.8.

Now that we have the values of the p_{d}, p_{fa} at respective error probabilities, we use the same to calculate and evaluate the power consumption and relative power saving in the next chapter.

Chapter 5

Power and Delay Analysis

Now that we have the expressions for average power calculation for the reference cases and our investigated solution, in both DRX and eDRX power saving modes along with the probability of detection, probability of false alarm values of the proposed WUS for the WRx, we calculate the relative power saving of MWUS and WWUS with respect to the No-WUS case.

5.1 Power Consumption, saving and dominant components analysis

In this section, we illustrate the average power consumption for the reference cases and the investigated case. For each case, we analyze the dominant components in the power consumption for both DRX and eDRX modes.

As our investigated WUS design is estimated to work well with bit error probabilities from 0.15 to 0.35 or MCL level from 144 dB to 149 dB, we restrict our comparisons of power consumption to the same MCL levels for better understanding.

For DRX cycle, different configurations of cycle time are possible. In our analysis, we consider the lowest and highest cycle times configurable for DRX cycle, 0.32 s and 2.56 s respectively. We have referred to the values enlisted in the tables 5.1 and 5.2 to calculate the power consumption in each case. From Figure 5.1, it is clear that the power consumption for MWUS is comparable to the power consumption in the No-WUS case for the MCL levels considered. For the WWUS, the results show lower power consumption compared to both the reference cases.

For eDRX cycles among the configurable cycle time possible, we choose, time periods 5.12 s and 2621.44 s. As observed in Figure 5.2, that WWUS has the lowest power consumption compared to the other cases. MWUS also shows lower power consumption than No-WUS case but not as low power consumption as WWUS.

Now, that we are aware of the power consumption in both the modes DRX and eDRX, and WWUS consumes the least power, we focus on the dominant energy cost components for all three cases. From Figure 5.3, we can easily infer that the transition energy and sleep time energy costs are the dominant components for No-WUS case during DRX cycle operation.

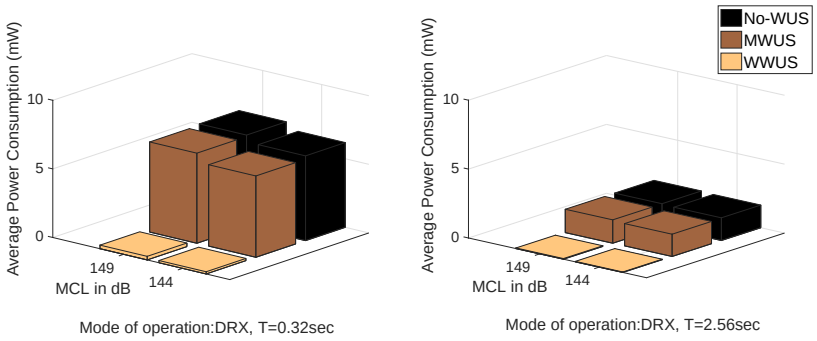

Figure 5.1: Average Power Consumption for No-WUS, MWUS and WWUS in DRX cycle

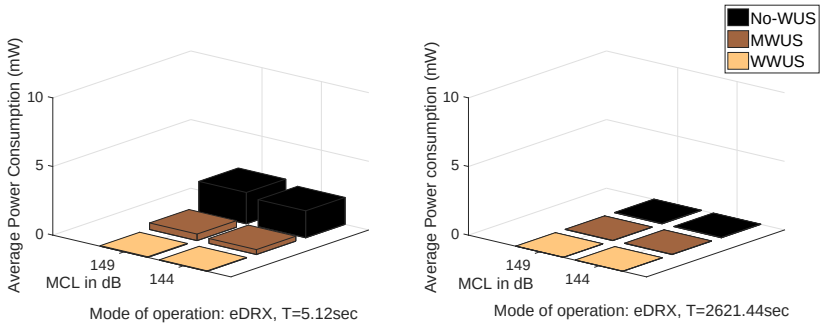

Figure 5.2: Average Power Consumption for No-WUS, MWUS and WWUS in eDRX cycle

In case of eDRX cycle, the energy cost components are shown in Figure 5.4. The larger cost components are idle listening and overhearing energy costs, i.e., no-paging and non-target paging energy costs. The light sleep contribution in the total energy cost is almost equivalent to non-target paging energy cost.

In case of MWUS during DRX cycle, as shown in Figure 5.5, the dominant cost components are mainly sleep time and transition energy, and the other energy costs are negligible compared to the overall energy cost.

During eDRX cycle, the MWUS solution has even distribution in terms of three dominant components namely, sleep, transition, sync and drift energy costs as shown in Figure 5.6.

From the above diagrams of energy cost distributions, we observe that, for the reference cases, the dominant components differ from each other during the

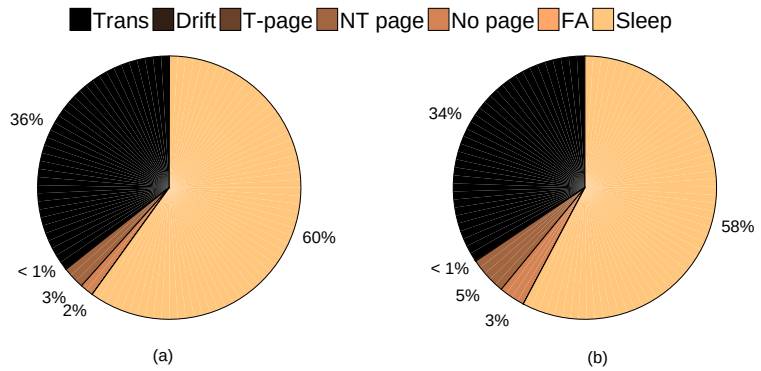

Figure 5.3: Energy consumption breakdown for No-WUS reference case during DRX cycle. (a) 144 dB MCL; (b)149 dB MCL

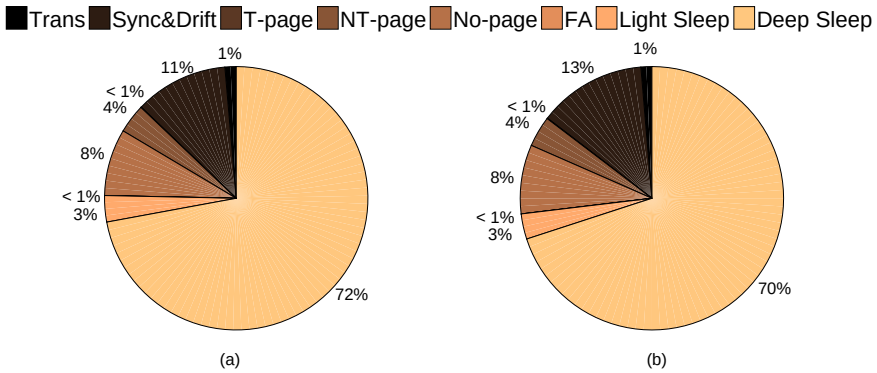

Figure 5.4: Energy consumption breakdown for No-WUS reference case during eDRX cycle. (a) 144 dB MCL; (b) 149 dB MCL

two power saving modes. During the DRX mode, the main energy cost driver for the reference cases are sleep and transition times. Transition energy is often overlooked by the receiver manufacturer but through this analysis, its importance is highlighted. In case of eDRX cycle, the energy cost bearers are mainly sync, drift, transition and deep sleep. Even during eDRX cycle, similar to DRX operation, transition energy continues to one of the dominant energy cost components while the synchronization cost is another heavy contributor in terms of energy consumption.

For the investigated solution, during DRX cycle, the individual energy cost components are shown in Figure 5.7. The dominant energy cost components are the transition, sync, drift and sleep time energy costs. As the UE ramps up from deep sleep to its ON state, the transition energy in WWUS solution shows notewor-

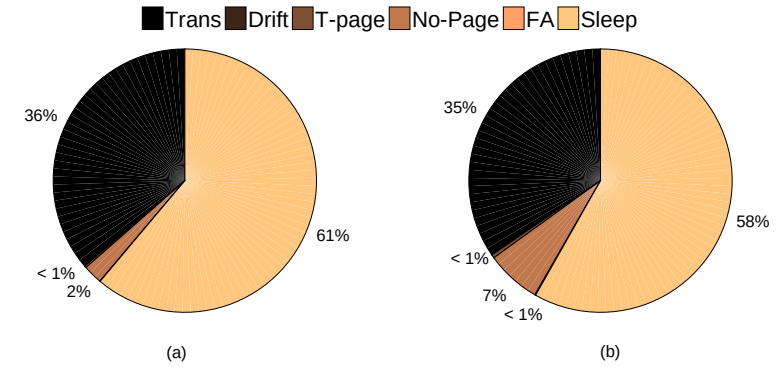

Figure 5.5: Energy consumption breakdown for MWUS reference case during DRX cycle. (a) 144 dB MCL; (b)149 dB MCL

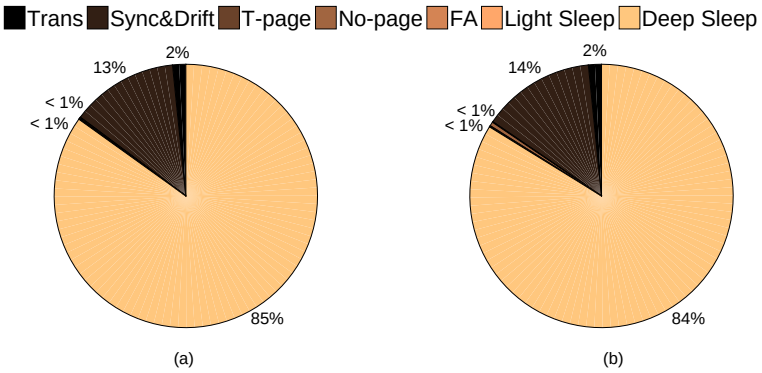

Figure 5.6: Energy consumption breakdown for MWUS reference case during eDRX cycle. (a) 144 dB MCL; (b)149 dB MCL

thy contribution on the overall energy consumption. While the WRx duty cycles on behalf of the MRx, in case of target paging, synchronization is unavoidable.

During the eDRX cycle, the WWUS solution shows minimum power consumption compared the reference cases. As the power consumption by the MRx is only when a target WUS is received, the UE sleeps for most of the time and hence saving more energy. The energy cost components with their contributions are shown in Figure 5.8.

The saving for WWUS in both the DRX and eDRX modes is so high compared to the reference cases but the dominant components remain the same as reference cases. The dominant components differ in magnitudes compared to the power consumption of the reference cases.

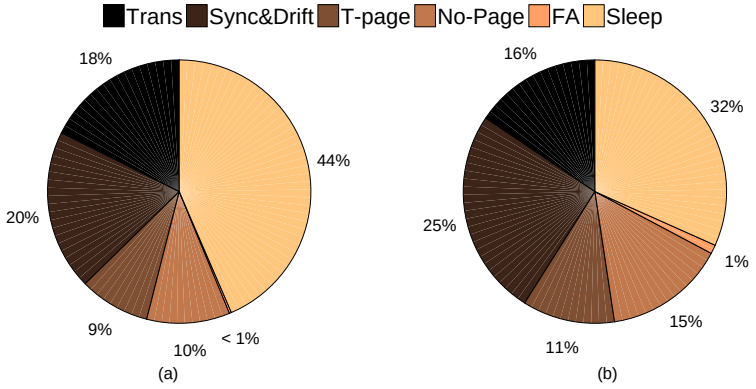

Figure 5.7: Energy consumption breakdown for WWUS case during DRX cycle. (a) 144 dB MCL; (b)149 dB MCL

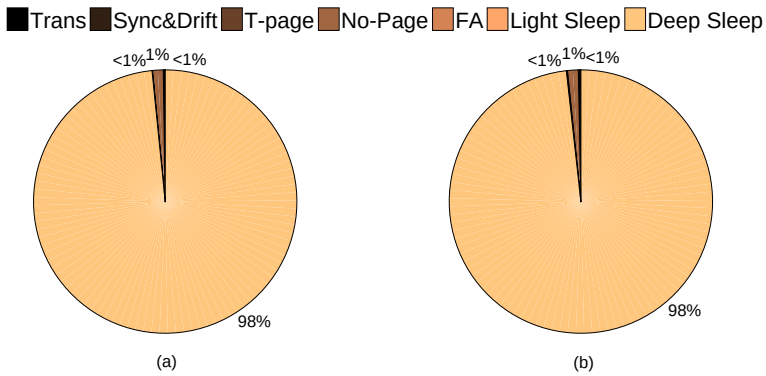

Figure 5.8: Energy consumption breakdown for WWUS case during eDRX cycle. (a) 144 dB MCL; (b)149 dB MCL

5.2 Power and Delay comparison

Now, after analyzing the power consumption and dominant cost components of the reference cases and the investigated solution in both DRX and eDRX modes of operation, we continue with the analysis of the power consumption with respect to delay. We have the respective power consumptions of a UE using different solutions. Now we calculate the delay using the equations derived in Chapter 3 and plot power consumption against the respective delays. The results are shown in the figures 5.9 and 5.10. From these figures, we observe that the WWUS solution is effective for both DRX and eDRX mode of operations. The situation during eDRX cycle is quite similar to the DRX operation in terms of power consumption with respect to delay analysis. From both the DRX and eDRX analysis, we can conclude that the power saving is more effective with shorter cycle times. In

case of longer configuration times, the sleep time is also longer which leads to a longer average delay. As the delay increases, the effect of power saving through WWUS solution reduces. Hence, it is preferred to use WWUS solution for the UEs configured with shorter cycle times.

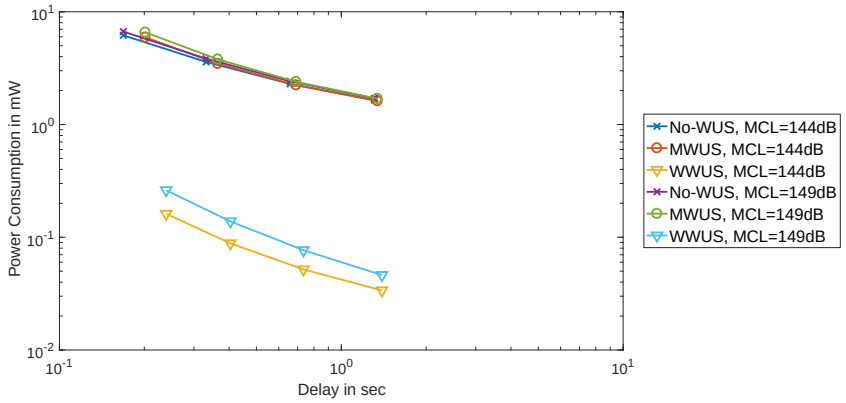

Figure 5.9: Power vs Delay Analysis for No-WUS, MWUS and WWUS case in DRX cycle

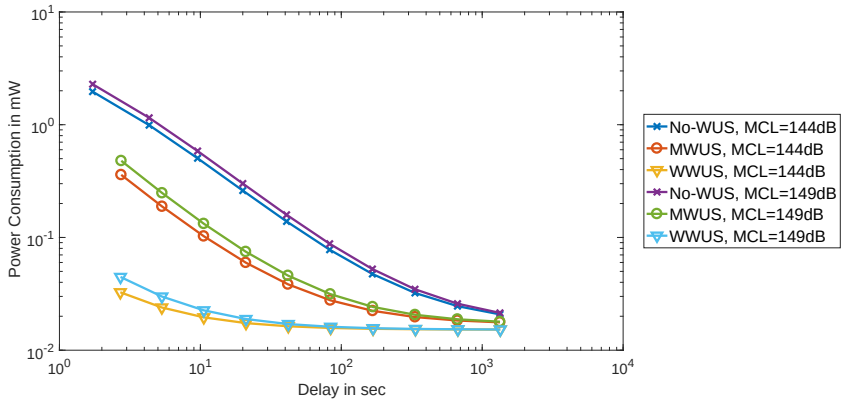

Figure 5.10: Power vs Delay Analysis for No-WUS, MWUS and WWUS case in eDRX cycle

Now, we continue our analysis to study the power saving with respect to MCL. In the WWUS case with DRX, within 149 dB MCL, 95% to 97% of power is saved with respect to the No-WUS case and it is much higher saving compared to the power saving achieved with the MWUS case with respect to the No-WUS case. The energy consumed in the MWUS case is almost equal to that of the No-WUS case at lower MCLs and achieves higher power saving at higher MCLs. In eDRX mode of operation, both the WWUS and MWUS solutions show significant amount of power saving. The MWUS solution shows a saving of around 80% compared

to the No-WUS case in the UEs duty cycling in eDRX cycles. WWUS gives a saving of nearly 98% at short eDRX cycles and around 25% at longer eDRX cycle cycles. In both the DRX and eDRX modes of operations, the WWUS solution, within 149 dB MCL is estimated to be a better solution than the considered reference cases. The power saving achieved with the MWUS and WWUS cases with respect to the No-WUS case for all the possible configuration cycle times are listed in Appendix, section A.2. The results obtained cannot be mapped with the battery life extension, as they reflect the energy saved in idle mode only. If the energy calculation of overall operation of UE is carried out and the percentage of idle mode energy out of the total consumption is known, then we can arrive at the exact amount of energy that would be saved. Hence, we have to express the average power saving relative to existing solutions.

The tables below specify all the variables we used in our calculations along with their descriptions and the values considered. The tables include all the power and time components, the probabilities used, signal repetitions and the error correction factors required for the drift time calculations.

Table 5.1: Power consumption and time values assumed from the references

[1], [5], [4], [6]

Notations	Description	Value(s)
P_{lrup}	MRx ramp up power from light sleep to ON	50mW
P_{M}	MRx power consumption	100mW
P_{lrdwn}	MRx ramp down power from ON to light sleep	50mW
P_{drup}	MRx ramp up power from deep sleep to ON	15mW
P_{drdwn}	MRx ramp down power from ON to deep sleep	15mW
P_{ds}	MRx deep sleep power consumption	0.015mW
P_{ls}	MRx light sleep power consumption	1mW
$P_{\text{rup}}^{\text{W}}$	WRx ramp up power from deep sleep to ON	0.15mW
P_{W}	WRx power consumption	100mW
$P_{\text{rdwn}}^{\text{W}}$	WRx ramp down power from ON to deep sleep	0.15mW
T^{drx}	Duration of duty cycles in DRX mode	[0.32,0.64, 1.28,2.56]s
T^{edrx}	Duration of duty cycles in eDRX mode	[5.12,10.24, 20.48,40.96, 81.92,163.84, 327.68,655.36, 1310.72,2621.44]s
T_{lrup}	MRx ramp up time from light sleep to ON	15ms
T_{lrdwn}	MRx ramp down time from ON to light sleep	15ms
T_{m}	Time required to read MPDCCH	1ms
T_{prt}	Time required for retuning to read PDSCH	1ms
T_{p}	Time required to read PDSCH	1ms
T_{ptw}	Duration of PTW	2.56ms
T_{drup}	MRx ramp up time from deep sleep to ON	25ms
T_{drdwn}	MRx ramp down time from ON to deep sleep	25ms
T_{sync}	Time required to acquire PSS and SSS	[10,22,40, 320,850]s
T_{bsync}	Time required to acquire RSS	1ms
T_{wus}	Time required to read WUS by MRx	1ms
$T_{\text{rup}}^{\text{W}}$	WRx ramp up time from deep sleep to ON	25ms
$T_{\text{rdwn}}^{\text{W}}$	WRx ramp down time from ON to deep sleep	25ms
$T_{\text{wus}}^{\text{W}}$	Time required to read WUS by WRx	1ms

Table 5.2: Probabilities, repetitions and drift calculation assumptions

Notations	Description	Value(s)
p_{d}	Probability of detection(ROC) of MRx	0.99
p_{p}	Probability of paging	0.3
p_{tp}	Probability of target paging	0.01
p_{ntp}	Probability of non-target paging	0.29
p_{fa}	Probability of paging false alarm in MRx	0.0001
p_{tgwus}	Probability of target group WUS	0.0188
$p_{\mathrm{d}}^{\mathrm{W}}$	Probability of detection(ROC) of WRx	0.979;0.996*
p_{fawus}	Probability of WUS false alarm in MRx	0.01
$p_{\mathrm{fawus}}^{\mathrm{W}}$	Probability of WUS false alarm in WRx	0.002;0.006*
n	No. of DRX cycles in 1 PTW	4
R_{m}	No. of MPDCCH repetitions w.r.t MCL	[1,2]*
R_{p}	No. of PDSCH repetitions w.r.t MCL	[2,4]*
R_{wus}	No. of WUS repetitions w.r.t MCL in MRx	[1,3]*
R_{bsync}	No. of repetitions required to resync w.r.t. MCL	[8,12]*
$R_{\mathrm{wus}}^{\mathrm{W}}$	No. of WUS repetitions w.r.t MCL in WRx	[1,10]*
e_{l}	Low correction factor for drift calculation in MRx	0.05
e_{h}	High correction factor for drift calculation in MRx	5
e_{rtc}	Real time clock correction factor for drift calculation in MRx	20
$e_{\mathrm{l}}^{\mathrm{W}}$	Low correction factor for drift calculation in WRx	0.5
$e_{\mathrm{h}}^{\mathrm{W}}$	Low correction factor for drift calculation in WRx	50
$e_{\mathrm{rtc}}^{\mathrm{W}}$	Real time clock correction factor for WRx	200

*The values are at MCLs 144 dB and 149 dB.

Chapter 6
Conclusions and Future Work

6.1 Conclusion

In this thesis work, we analyzed the feasibility of using a wake-up receiver in the existing receiver circuitry to save power during the idle mode of operation. We first calculated the power consumption for two reference cases, in the first case, there is no concept of wake-up signal and in the second case, wake up signal has been introduced to be received by the main receiver. When we compared the power saving of the investigated solution during discontinuous reception mode of operation with the first reference case, it is expected to save sixteen to seventy-nine percent of the power consumption, whereas, in case of extended discontinuous reception mode of operation, the investigated solution is expected to save twenty-six to ninety-eight percent of power consumption. The percentage varies with the configured cycle times. Now, when we compare the same with the second reference case, the relative saving is ninety-six to ninety-eight percent during discontinuous reception mode and in case of extended discontinuous reception mode, the relative power saving varies from thirteen to ninety-one percent depending on the cycle time selected. We also analyzed the dominant components in both reference cases and the investigated solution, and arrived at the conclusion that the transition, synchronization and drift energy costs are expected to be dominant in most of the cases. Further saving can be achieved, if the transition and synchronization energy costs are lowered. Comparing the power consumption with respect to delay in both the modes of operation, we found that the investigated solution is more effective in power saving for short cycles. Moreover, the design of wake up signal has been estimated to work well within the range of maximum coupling loss, 149 dB. In case, power boosting is applied in the future, the same design can be used for an extended maximum coupling loss range with respect to the magnitude of power boost applied.

In our energy consumption calculations, mobility aspect is not included for simplicity. In both the power saving modes, the investigated solution is evaluated to be an effective solution. We have adapted a certain technique to optimize the energy saving during idle mode operation of a device, but there can be other techniques to optimize the energy saving as well. Different approach towards the design of wake-up signal may also prove more beneficial but it demands more research work. Due to the limitation on time, we have limited ourselves to this

point and discuss the future work in the next section.

6.2 Future Work

There are lots of open areas to research within this area of study. To start with, from the energy calculation perspective, the equations derived can be revised to include the mobility of UE. From the WUS design perspective, addressing the individual UEs with a WUS is an open topic of research to completely eradicate the overhearing energy cost. With the WUS designs proposed, simulations were carried out up to bit error probability of 0.35 and research work can be continued for higher bit error probabilities to find and propose its usability in case of maximum coupling loss higher than 149 dB.

Appendix A

Sleep time calculations and Relative power saving

A.1 Light and Deep Sleep Calculations

Here, we list the equations for light and deep sleep time calculations which are used in Chapter 3.

A.1.1 DRX - Sleep time calculations

No-WUS:

$$\begin{aligned} T_{\text{ls}}^{\text{drx}} =& T^{\text{drx}} - \big[T_{\text{lrup}} + T_{\text{ls-drift}} + T_{\text{m}} R_{\text{m}} \\ &+ [p_{\text{p}} \cdot p_{\text{d}} + (1 - p_{\text{p}}) p_{\text{fa}}](T_{\text{prt}} + T_{\text{p}} R_{\text{p}}) \\ &+ T_{\text{lrdwn}}\big] \end{aligned} \tag{A.1}$$

MWUS:

$$\begin{aligned} T_{\text{ls}}^{\text{drx}} =& T^{\text{drx}} - \big[T_{\text{lrup}} + T_{\text{ls-drift}} + T_{\text{wus}} R_{\text{wus}} \\ &+ p_{\text{tgwus}} \cdot p_{\text{d}}^{\text{mwus}} (T_{\text{m}} R_{\text{m}} + T_{\text{prt}} + T_{\text{p}} R_{\text{p}}) \\ &+ (1 - p_{\text{tgwus}}) p_{\text{fa}} \cdot T_{\text{m}} R_{\text{m}} \\ &+ T_{\text{lrdwn}}\big] \end{aligned} \tag{A.2}$$

WWUS:

$$T_{\text{on}}^{\text{W}} = T_{\text{rup}}^{\text{W}} + T_{\text{drift}}^{\text{W}} + T_{\text{wus}}^{\text{W}} R_{\text{wus}}^{\text{W}} + T_{\text{rdwn}}^{\text{W}} \tag{A.3}$$

$$\begin{aligned} T_{\text{ds}}^{\text{drx}} =& T^{\text{drx}} - \big[T_{\text{on}}^{\text{W}} + p_{\text{tgwus}} \cdot p_{\text{d}}^{\text{W}} (T_{\text{drup}} + T_{\text{ds-drift}} \\ &+ T_{\text{bsync}} R_{\text{bsync}} + T_{\text{m}} R_{\text{m}} + T_{\text{prt}} + T_{\text{p}} R_{\text{p}} + T_{\text{drdwn}}) \\ &+ (1 - p_{\text{tgwus}}) p_{\text{faw us}}^{\text{W}} (T_{\text{drup}} + T_{\text{ds-drift}} \\ &+ T_{\text{bsync}} R_{\text{bsync}} + T_{\text{m}} R_{\text{m}} + T_{\text{drdwn}})\big] \end{aligned} \tag{A.4}$$

A.1.2 eDRX - Light sleep time calculations

No-WUS:

$$
\begin{aligned}
T_{\text{ls}}^{\text{edrx}} =& p_{\text{tp}} \frac{(\alpha)(1-\alpha)}{(1-\alpha^n)} \Big[(1+2\alpha+3\alpha^2)\big[T^{\text{idrx}} - (T_{\text{lrup}} + T_{\text{ls-drift}} + T_{\text{m}} R_{\text{m}} + T_{\text{lrdwn}})\big] \\
& - (1+\alpha+2\alpha^2)(T_{\text{sync}} R_{\text{sync}} + T_{\text{ds-drift}} - T_{\text{ls-drift}}) \Big] \\
& + p_{\text{ntp}} \frac{(1-\alpha)}{(1-\alpha^n)} \Big[(1+\alpha+2\alpha^2)\big[3T^{\text{idrx}} - 3(T_{\text{lrup}} + T_{\text{ls-drift}} + T_{\text{m}} R_{\text{m}} + T_{\text{lrdwn}}) \\
& - (T_{\text{prt}} + T_{\text{p}} R_{\text{p}})\big] + 3\alpha^3\big[T^{\text{idrx}} - (T_{\text{lrup}} + T_{\text{ls-drift}} + T_{\text{m}} R_{\text{m}} + T_{\text{lrdwn}})\big] \\
& - (T_{\text{sync}} R_{\text{sync}} + T_{\text{ds-drift}} - T_{\text{ls-drift}}) \Big] \\
& + (1-p_{\text{p}})(1-p_{\text{fa}}) \Big[(n-1)\big[T^{\text{idrx}} - (T_{\text{lrup}} + T_{\text{ls-drift}} + T_{\text{m}} R_{\text{m}} + T_{\text{lrdwn}})\big] \\
& - (T_{\text{sync}} R_{\text{sync}} + T_{\text{ds-drift}} - T_{\text{ls-drift}}) \Big] \\
& + (1-p_{\text{p}}) p_{\text{fa}} \Big[(n-1)\big[T^{\text{idrx}} - (T_{\text{lrup}} + T_{\text{ls-drift}} + T_{\text{m}} R_{\text{m}} + T_{\text{prt}} + T_{\text{p}} R_{\text{p}} \\
& + T_{\text{lrdwn}})\big] - (T_{\text{sync}} R_{\text{sync}} + T_{\text{ds-drift}} - T_{\text{ls-drift}}) \Big]
\end{aligned}
\tag{A.5}
$$

MWUS:

$$
\begin{aligned}
T_{\text{ls}}^{\text{edrx}} =& p_{\text{d}}^{\text{mwus}} \cdot p_{\text{tgwus}} \frac{(\alpha)(1-\alpha)}{(1-\alpha^n)} \Big[(1+2\alpha+3\alpha^2)\big[T^{\text{idrx}} - (T_{\text{lrup}} + T_{\text{ls-drift}} + T_{\text{m}} R_{\text{m}} \\
& + T_{\text{lrdwn}})\big] - (1+\alpha+2\alpha^2)(T_{\text{wus}} R_{\text{wus}} + T_{\text{bsync}} R_{\text{bsync}} + T_{\text{ds-drift}} - T_{\text{ls-drift}}) \Big] \\
& + (1-p_{\text{tgwus}}) p_{\text{fawus}} \Big[(n-1)\big[T^{\text{idrx}} - (T_{\text{lrup}} + T_{\text{ls-drift}} + T_{\text{m}} R_{\text{m}} + T_{\text{lrdwn}})\big] \\
& - (T_{\text{wus}} R_{\text{wus}} + T_{\text{sync}} R_{\text{sync}} + T_{\text{ds-drift}} - T_{\text{ls-drift}}) \Big]
\end{aligned}
\tag{A.6}
$$

WWUS:

$$
\begin{aligned}
T_{\text{ls}}^{\text{edrx}} =& p_{\text{tgwus}} \cdot p_{\text{d}}^{\text{W}} \frac{(\alpha)(1-\alpha)}{(1-\alpha^n)} \Big[(1+2\alpha+3\alpha^2)\big[T^{\text{idrx}} - (T_{\text{lrup}} + T_{\text{ls-drift}} + T_{\text{m}} R_{\text{m}} \\
& + T_{\text{lrdwn}})\big] - (1+\alpha+2\alpha^2)(T_{\text{bsync}} R_{\text{bsync}} + T_{\text{ds-drift}} - T_{\text{ls-drift}}) \Big] \\
& + (1-p_{\text{tgwus}}) p_{\text{fawus}}^{\text{W}} \Big[(n-1)\big[T^{\text{idrx}} - (T_{\text{lrup}} + T_{\text{ls-drift}} + T_{\text{m}} R_{\text{m}} + T_{\text{lrdwn}})\big] \\
& - (T_{\text{sync}} R_{\text{sync}} + T_{\text{ds-drift}} - T_{\text{ls-drift}}) \Big]
\end{aligned}
\tag{A.7}
$$

A.1.3 eDRX - Deep sleep time calculations

No-WUS:

$$
\begin{aligned}
T_{\text{on}}^{\text{edrx}} =& p_{\text{tp}}\Bigg[\left(\frac{n\alpha^{n+1}-(n+1)\alpha^{n}+1}{(1-\alpha^{n})(1-\alpha)}\right)(T_{\text{lrup}}+T_{\text{ls-drift}}+T_{\text{m}}R_{\text{m}} \\
&+T_{\text{lrdwn}})+(T_{\text{prt}}+T_{\text{p}}R_{\text{p}})+(T_{\text{sync}}R_{\text{sync}}+T_{\text{ds-drift}}-T_{\text{ls-drift}}) \\
&+\frac{(\alpha)(1-\alpha)}{(1-\alpha^{n})}\big[(1+2\alpha+3\alpha^{2})[T^{\text{idrx}}-(T_{\text{lrup}}+T_{\text{ls-drift}}+T_{\text{m}}R_{\text{m}}+T_{\text{lrdwn}})] \\
&-(1+\alpha+\alpha^{2})(T_{\text{sync}}R_{\text{sync}}+T_{\text{ds-drift}}-T_{\text{ls-drift}})\big]\Bigg] \\
&+p_{\text{ntp}}\Bigg[n(T_{\text{lrup}}+T_{\text{ls-drift}}+T_{\text{m}}R_{\text{m}}+T_{\text{lrdwn}}) \\
&+p_{\text{d}}\cdot(T_{\text{prt}}+T_{\text{p}}R_{\text{p}})+(T_{\text{sync}}R_{\text{sync}}+T_{\text{ds-drift}}-T_{\text{ls-drift}}) \\
&+\frac{(1-\alpha)}{(1-\alpha^{n})}\big[(1+\alpha+2\alpha^{2})[3T^{\text{idrx}}-3(T_{\text{lrup}}+T_{\text{ls-drift}}+T_{\text{m}}R_{\text{m}}+T_{\text{lrdwn}}) \\
&-(T_{\text{prt}}+T_{\text{p}}R_{\text{p}})]+3\alpha^{3}[T^{\text{idrx}}-(T_{\text{lrup}}+T_{\text{ls-drift}}+T_{\text{m}}R_{\text{m}}+T_{\text{lrdwn}})] \\
&-(T_{\text{sync}}R_{\text{sync}}+T_{\text{ds-drift}}-T_{\text{ls-drift}})\big]\Bigg] \\
&+(1-p_{\text{p}})(1-p_{\text{fa}})\Bigg[n(T_{\text{lrup}}+T_{\text{ls-drift}}+T_{\text{m}}R_{\text{m}}+T_{\text{lrdwn}}) \\
&+(n-1)\big[T^{\text{idrx}}-(T_{\text{lrup}}+T_{\text{ls-drift}}+T_{\text{m}}R_{\text{m}}+T_{\text{lrdwn}})\big]\Bigg] \\
&+(1-p_{\text{p}})p_{\text{fa}}\Bigg[n(T_{\text{lrup}}+T_{\text{ls-drift}}+T_{\text{m}}R_{\text{m}}+T_{\text{lrdwn}}+T_{\text{prt}}+T_{\text{p}}R_{\text{p}}) \\
&+(n-1)\big[T^{\text{idrx}}-(T_{\text{lrup}}+T_{\text{ls-drift}}+T_{\text{m}}R_{\text{m}}+T_{\text{prt}}+T_{\text{p}}R_{\text{p}}+T_{\text{lrdwn}})\big]\Bigg]
\end{aligned}
\tag{A.8}
$$

$$
T_{\text{ds}}^{\text{edrx}} = T^{\text{edrx}} - (T_{\text{drup}} + T_{\text{on}}^{\text{edrx}} + T_{\text{drdwn}}) \tag{A.9}
$$

MWUS:

$$\begin{aligned}
T_{\text{on}}^{\text{edrx}} =& p_{\text{d}}^{\text{mwus}} \cdot p_{\text{tgwus}} \Big[T_{\text{ds-drift}} + T_{\text{bsync}} R_{\text{bsync}} \\
& - T_{\text{ls-drift}} + T_{\text{wus}} R_{\text{wus}} - (T_{\text{lrup}} + T_{\text{lrdwn}}) \\
& + \left(\frac{n\alpha^{n+1} - (n+1)\alpha^n + 1}{(1-\alpha^n)(1-\alpha)} \right) (T_{\text{lrup}} + T_{\text{ls-drift}} + T_{\text{m}} R_{\text{m}} \\
& + T_{\text{lrdwn}}) + T_{\text{prt}} + T_{\text{p}} R_{\text{p}} \\
& + \frac{(\alpha)(1-\alpha)}{(1-\alpha^n)} \big[(1 + 2\alpha + 3\alpha^2) \big[T^{\text{idrx}} - (T_{\text{lrup}} + T_{\text{ls-drift}} + T_{\text{m}} R_{\text{m}} \\
& + T_{\text{lrdwn}}) \big] - (1 + \alpha + 2\alpha^2)(T_{\text{wus}} R_{\text{wus}} + T_{\text{bsync}} R_{\text{bsync}} + T_{\text{ds-drift}} \\
& - T_{\text{ls-drift}}) \big] \Big] + [p_{\text{tgwus}}(1 - p_{\text{d}}^{\text{mwus}}) + (1 - p_{\text{tgwus}}) p_{\text{fawus}}] (T_{\text{ds-drift}} \\
& + T_{\text{bsync}} R_{\text{bsync}} + T_{\text{wus}} R_{\text{wus}}) \\
& + (1 - p_{\text{tgwus}}) p_{\text{fawus}} \big[n(T_{\text{lrup}} + T_{\text{ls-drift}} + T_{\text{m}} R_{\text{m}} + T_{\text{lrdwn}} - (T_{\text{lrup}} \\
& + T_{\text{lrdwn}}) + (n-1)[T^{\text{idrx}} - (T_{\text{lrup}} + T_{\text{ls-drift}} + T_{\text{m}} R_{\text{m}} + T_{\text{lrdwn}})] \big]
\end{aligned} \tag{A.10}$$

$$T_{\text{ds}}^{\text{edrx}} = T^{\text{edrx}} - (T_{\text{drup}} + T_{\text{on}}^{\text{edrx}} + T_{\text{drdwn}}) \tag{A.11}$$

WWUS:

$$\begin{aligned}
T_{\text{on}}^{\text{edrx}} =& p_{\text{tgwus}} \cdot p_{\text{d}}^{\text{W}} \Big[T_{\text{on}}^{\text{W}} + T_{\text{drup}} + T_{\text{ds-drift}} + T_{\text{bsync}} R_{\text{bsync}} \\
& + \big[\left(\frac{n\alpha^{n+1} - (n+1)\alpha^n + 1}{(1-\alpha^n)(1-\alpha)} \right) (T_{\text{lrup}} + T_{\text{ls-drift}} + T_{\text{m}} R_{\text{m}} \\
& + T_{\text{lrdwn}}) + T_{\text{prt}} + T_{\text{p}} R_{\text{p}} \big] - (T_{\text{ls-drift}} + T_{\text{lrup}} + T_{\text{lrdwn}}) + T_{\text{drdwn}} \\
& + \frac{(\alpha)(1-\alpha)}{(1-\alpha^n)} \big[(1 + 2\alpha + 3\alpha^2) \big[T^{\text{idrx}} - (T_{\text{lrup}} + T_{\text{ls-drift}} + T_{\text{m}} R_{\text{m}} \\
& + T_{\text{lrdwn}}) \big] - (1 + \alpha + 2\alpha^2)(T_{\text{bsync}} R_{\text{bsync}} + T_{\text{ds-drift}} - T_{\text{ls-drift}}) \big] \Big] \\
& + [p_{\text{tgwus}}(1 - p_{\text{d}}^{\text{W}}) + (1 - p_{\text{tgwus}})(1 - p_{\text{fawus}}^{\text{W}})] T_{\text{on}}^{\text{W}} \\
& + (1 - p_{\text{tgwus}}) p_{\text{fawus}}^{\text{W}} \Big[T_{\text{on}}^{\text{W}} + T_{\text{drup}} + T_{\text{ds-drift}} + T_{\text{bsync}} R_{\text{bsync}} \\
& + n(T_{\text{lrup}} + T_{\text{ls-drift}} + T_{\text{m}} R_{\text{m}} + T_{\text{lrdwn}}) \\
& - (T_{\text{ls-drift}} + T_{\text{lrup}} + T_{\text{lrdwn}}) + T_{\text{drdwn}} \\
& + (n-1) \big[T^{\text{idrx}} - (T_{\text{lrup}} + T_{\text{ls-drift}} + T_{\text{m}} R_{\text{m}} + T_{\text{lrdwn}}) \big] \\
& - (T_{\text{sync}} R_{\text{sync}} + T_{\text{ds-drift}} - T_{\text{ls-drift}}) \Big]
\end{aligned} \tag{A.12}$$

$$T_{\text{ds}}^{\text{edrx}} = T^{\text{edrx}} - T_{\text{on}}^{\text{edrx}} \tag{A.13}$$

A.2 Relative Power Saving

Here, we show the relative power saving achieved with the MWUS and WWUS cases with respect to the No-WUS case.

Table A.1: Power saving with MWUS case in DRX mode of operation

Cycle time	144 dB MCL (in %)	149 dB MCL (in %)
0.32	4.04	1.55
0.64	3.47	1.35
1.28	2.72	1.07
2.56	1.89	0.75

Table A.2: Power saving with WWUS case in DRX mode of operation

Cycle time	144 dB MCL (in %)	149 dB MCL (in %)
0.32	97.38	96.08
0.64	97.53	96.39
1.28	97.73	96.82
2.56	97.95	97.29

Table A.3: Power saving with MWUS case in eDRX mode of operation

Cycle time	144 dB MCL (in %)	149 dB MCL (in %)
5.12	81.72	79.07
10.24	81.02	78.49
20.48	79.66	77.35
40.96	72.33	71.13
81.92	77.06	75.16
163.84	64.44	64.25
327.68	52.88	53.83
655.36	38.91	40.64
1310.72	25.44	27.25
2621.44	15.01	16.40

Table A.4: Power saving with WWUS case in eDRX mode of operation

Cycle time	144 dB MCL (in %)	149 dB MCL (in %)
5.12	98.33	98.04
10.24	97.58	97.40
20.48	96.11	96.13
40.96	93.32	93.71
81.92	88.25	89.26
163.84	79.77	81.65
327.68	67.36	70.12
655.36	52.35	55.52
1310.72	37.88	40.71
2621.44	26.68	28.70

References

[1] 3GPP. R1-1714992, Assumptions for eMTC Power Consumption for Power Saving Signal/Channel, RAN WG1 Meeting 90, Prague, Czech Republic, 21st-25th August, 2017.

[2] 3GPP. Evolved Universal Terrestrial Radio Access (E-UTRA); Physical channels and modulation, Release 15, 2018.

[3] 3GPP. Evolved Universal Terrestrial Radio Access (E-UTRA), Physical layer procedures, Release 15, 2018.

[4] 3GPP. R1-1807102, Reduce system acquisition time, RAN1 Meeting 93, Busan, Korea, May 21st – 25th, 2018.

[5] 3GPP. R1-1807104, WUS for MTC, RAN1 Meeting 93, Busan, Korea, May 21st – 25th, 2018.

[6] Erik Dahlman, Stefan Parkvall, and Johan Skold. *4G, LTE-advanced Pro and the Road to 5G*. Academic Press, 3 edition, 2016.

[7] Nour Kouzayha, Zaher Dawy, and Jeffrey G Andrews. Analysis of a power efficient wake-up solution for m2m over cellular using stochastic geometry. In *Global Communications Conference (GLOBECOM), 2016 IEEE*, pages 1–7. IEEE, 2016.

[8] Nafiseh Seyed Mazloum and Ove Edfors. Performance analysis and energy optimization of wake-up receiver schemes for wireless low-power applications. *IEEE Transactions on Wireless Communications*, 13(12):7050–7061, 2014.

[9] Nafiseh Seyed Mazloum and Ove Edfors. Influence of duty-cycled wake-up receiver characteristics on energy consumption in single-hop networks. *IEEE Transactions on Wireless Communications*, 16(6):3870–3884, 2017.